Spring 2023

An Investigation into Aluminum's Torsional Behavior of Circular, Rectangular, and Square Cross-Sections

Marly McClintock
msm042@bucknell.edu

Follow this and additional works at: https://digitalcommons.bucknell.edu/honors_theses

Part of the Structural Engineering Commons

An Investigation into Aluminum's Torsional Behavior of Circular, Rectangular, and Square Cross-Sections

By

Margaret S. McClintock
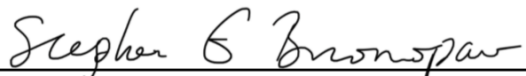
A Thesis Submitted to the Honors Council
For Honors in the Department of Civil and Environmental Engineering

May 2023

Approved by:

Advisor: Dr. Ronald D. Ziemian
Department of Civil and Environmental Engineering

Second Reader: Dr. Stephen Buonopane
Department of Civil and Environmental Engineering

Department Chair: Dr. Michael Malusis
Department of Civil and Environmental Engineering

Honors Council Representative: Dr. Michael Reeks
Department of Mathematics

ACKNOWLEDGEMENTS

First, I would like to thank Professor Ronald D. Ziemian for guiding me through this entire process and granting me so many amazing opportunities as an undergraduate. He introduced me to the world of aluminum design and instilled a standard of excellence that I will continue to embody post Bucknell.

Next, I would like to thank the other members of my defense committee, Professor Stephen Buonopane and Professor Michael Reeks, for evaluating my research and providing valuable feedback.

This research would not have been possible without the efforts of Jim Gutelius, the Civil Engineering Laboratories Director. Thank you for preparing all of the test specimens and helping me in the lab whenever necessary.

A special thanks to my family, particularly my parents, Dave and Sarah, and brother, Ridge, for their constant support throughout this endeavor. You have always been there for me, and I would not be the person that I am today without you.

Finally, I would like to thank all of my friends for making this research and my time at Bucknell so memorable. You all hold a special place in my heart.

TABLE OF CONTENTS

LIST OF TABLES

LIST OF FIGURES

ABSTRACT

The *Specifications for Aluminum Structures* (2020) provides the standards that structural engineers follow for aluminum design. Included in these specifications are limit state equations that use strength properties to calculate a member's initial yield, full yield, and rupture values. One limit state that the standards currently neglect is the torsional failure of solid bars. Torsion is the act of rotation caused by a twisting force, otherwise known as torque. Future installments of the specifications hope to include torsional yielding and rupture equations, so this study investigates the validity of these proposed equations.

Two different aluminum alloys were investigated for this research: 6061-T6 and 5052-H32. Both alloys are common structural material. In order to employ the proposed limit state equations, these alloys underwent torsion and tension testing. The results of tension tests are displayed first, followed by the results of the torsion tests. Furthermore, each section divides the results according to the alloy of interest. The experimental strength properties determined from tension testing and the strength properties listed in the specifications were used to evaluate the torsional limit states. The yielding predictions, initial and full, were plotted with the torsion results in order to assess the legitimacy of the equations. The rupture predictions used table comparisons to assess the accuracy of the equations. Statistical analyses were conducted on the results to support the experimental findings. The results of both alloys confirmed that the proposed limit state equations for torsion are accurate. However, concerns were raised because the *Specifications for Aluminum Structures* appeared to overestimate the strength properties of the 5052-H32 alloy. Therefore, it was concluded that the equations are accurate, but the yield and ultimate strength values listed in the *Aluminum Design Manual* (2020) require further investigation. Recommendations for future work are also provided within this thesis.

CHAPTER 1: INTRODUCTION AND LITERATURE REVIEW

1.1 Thesis Statement

The "Specifications for Aluminum Structures" should implement the proposed limit state equations for torsional yielding and rupture in the next installment of the Aluminum Design Manual because the equations accurately predict an alloy's torsional failure modes.

1.2 Introduction

Structural engineering projects are large-scale endeavors, and as such, the profession rarely has the opportunity during the design process to implement the fabrication and experimental testing of full-scale prototypes. Such undertakings would be highly costly and time consuming. As a result, building codes have been established to create a "rulebook" for engineers to follow when designing structural systems for safety. The specific details of these codes vary by material with different codes typically provided for reinforced concrete, steel, aluminum, and wood. Regarding metal systems, most structural engineers are well versed in the design of steel structures, but often struggle when transitioning to aluminum design because they may rarely employ this material. It is further noted that all material standards are constantly re-evaluated to ensure not only their accuracy, but also their ease of use. It is essential that such rules are applied per the intent of the code – an incorrect interpretation could lead to a major structural failure.

Within each code lie equations that are used to calculate a material's possible failure modes. These equations are called limit states and typically evaluate a material's initial yield, full yield, and

rupture values. One possible failure mode to consider is torsional failure. Torsion is the result of a force being applied to a member that in turn induces rotation. Torque, a twisting force that produces rotation about a particular axis, creates torsion and generates a shear stress over a specimen's cross-section. Limit state equations for torsional failure of bars do not currently exist in the code used for aluminum design.

The Aluminum Design Manual contains the *Specifications for Aluminum Structures*. These specifications were first published in November of 1967 and installments were published every five years following this initial release. However, the next publication is expected to be released in 2026, following the American Institute of Steel Construction's (AISC) six-year release schedule. The specification was reconstructed in 2010 to adopt AISC's *Specification for Structural Steel Buildings* structure (Kissell, Ziemian - 2020). The purpose of this reformatting was to simplify the process of switching between these two specifications. In essence, once the process to design steel structures is learned, the same methodology applies to aluminum design and vice versa.

This thesis will focus on evaluating the accuracy of proposed torsion equations that may be inserted into the *Specifications for Aluminum Structures*.

1.3 Purpose and Objectives

Aluminum structural design is on the rise as the metal's recyclability, high strength-to-weight ratio, and corrosion resistant properties make the material structurally appealing. As a result, the aluminum specifications need to include all potential limit states that could lead to a structural

failure. The *Specifications for Aluminum Structures* currently cover the design of members for tension, compression, flexure, combined forces, and torsion. However, the torsion section, H.2, shares a chapter with combined forces and provides unclear instructions on how to find the limit states, particularly for rectangular shaped cross-sections. In fact, the specification disregards solid bars entirely from the torsion section (Aluminum Association, 2020). This lack of emphasis on torsional limit state equations suggest that the specifications may be overly conservative, resulting in an excessive use of material and an increased total cost.

The primary objectives of the experimental research include the following:

- Understand torsional behavior at initial yield, full yield, and rupture.
- Collect torsion data so that the predicted limit state values can be compared to experimental torsion data. These predictions will be calculated using the initial yield and ultimate strength values discovered through two different methods:
    o The strength values listed in the *Specification for Aluminum Structures.*
    o The strength values determined through tension testing on alloy material.
- Propose modifications for the next installment of the Aluminum Design Manual.

1.4 Background

Aluminum alloys are metal mixtures that have a unique chemical composition. The primary metals that are added to the aluminum include copper, manganese, magnesium, silicon, and zinc. The presence of these other elements imparts various material characteristics such as increased strength, improved resistance to corrosion, and more ductility (Kissell, Ferry - 2002). Without

aluminum alloys, the metal would be incapable of being used for structural applications because pure aluminum is simply not strong enough to support a structure's design loads.

These alloys are then subdivided into two categories: wrought and cast alloys. For wrought alloys, each alloy is assigned a four-digit code that is used to differentiate between the different alloys. The first number designates the primary alloying group, which is a group of alloys that shares similar properties. The Aluminum Association currently recognizes nine different alloy groups. The 6XXX series is the most popular among structural engineers. The second number illustrates a modification to a primary alloy. For example, 6463 is a modified 6063 alloy that slightly alters the alloy's chemical composition so that better finishing characteristics are achieved. The last two numbers are sequentially assigned by the Aluminum Association based on the order that the association registers them. There are 357 registered alloys; however, the specification only includes 22, which indicates that a small percentage of these alloys are regularly used for structural design (Kissell, Ferry - 2002).

The numbers and letters that follow the four-digit code indicate an alloy's temper, which means that either heat treating or strain hardening methods were applied to the alloy. In terms of heat treatment, two techniques may be applied to the aluminum. Both processes begin at the annealed stage, which is when the metal is in its weakest, yet most ductile state. The aluminum is then quenched. Quenching is when the alloying element is quickly cooled in a controlled environment. The first form of heat treatment involves artificial aging. To artificially age an alloy, after rapidly heating and quenching the element of interest, the aluminum is heated to a slightly higher temperature, held there for a controlled number of hours, then brought back to room temperature. The other temperature effect possibility, natural aging, follows a similar procedure; however, this

colling process happens at room temperature. As a result, natural aging is more time-consuming because the cooling occurs more slowly than artificial aging. A capital *T* follows the alloy grouping number when the alloy underwent either temperature tempering processes. Heat treatment is typically only applicable to the 2XXX, 6XXX, and 7XXX series due to their chemical compositions (Kissell, Ferry - 2002).

An alternative temper operation practiced on aluminum alloys is strain hardening. Another common name for this process is cold working. Essentially, the aluminum is rolled at room temperature to achieve a certain thickness. The rolling decreases the alloy's ductility and increases its total strength. Strain-hardened alloys are denoted by placing an *H* after the four-digit code. The number(s) that follow help further classify the alloy. The first number categorizes the aluminum into one of the four different strained-hardened tempers. The second digit denotes the degree of strain-hardening. A cold-worked alloy with a second number of 8 signals that the alloy possesses the largest ultimate strength value that is accepted and implemented by the structural engineering community. This classification is often termed *full-hard*. A 1 rarely appears in the description because this value corresponds to the annealed state in which the letter *O* depicts this temper instead.

6061-T6 and 5052-H32 were the two alloys selected to conduct this study. Both alloys are common forms of aluminum used for structural applications. ASTM standards currently exist for 6061-T6 structural profiles but do not exist for the 5052-H32 alloy. The full text of this standard can be found in the appendix (ASTM 02.02). 6061-T6 aluminum was developed by the Aluminum Company of America in 1935 (Simcoe, 2011). This alloy contains aluminum, magnesium, and

silicon and exhibits excellent machinability and weldability while simultaneously maintaining high strength characteristics. This alloy undergoes artificial aging, which is indicated by the *T* in the alloy description. In order to achieve the T6 temper the 6061 alloy is heated to 990°F, rapidly quenched, heated again to 320°F and held at that temperature for eighteen hours. Finally, the aluminum is cooled to room temperature (Kissell, Ferry - 2002).

H32 tempers apply to products that are cold-worked and experience some thermal treatment to stabilize the mechanical properties. The second digit, 2, implies that the alloy is *quarter-hard*. In other words, the tensile strength is one-fourth the *full hard* strength (Kissell, Ferry - 2002).

1.5 Thesis Overview and Organization

This thesis is organized into seven chapters. Chapter 1 introduces the thesis topic, explains the purpose of this study, and provides relevant background information. Chapter 2 covers a theoretical review and derivation of the equations that were used for this research. Chapter 3 presents all of the procedures and results of the tension and torsion testing. Chapter 4 summarizes the experimental results. Chapter 5 examines the results, lists conclusions of the study, acknowledges the research's limitations, and suggests possibilities for additional research. The thesis concludes with the bibliography and appendix.

CHAPTER 2: THEORETICAL REVIEW

In order to compute the theoretical torque values predicted for each aluminum alloy, the torsion equations needed to be rearranged so that limit state equations for torque could be derived. These derivations include initial yielding, full yielding, and rupture. The following sections will outline the process taken to achieve the final equations that were ultimately used to make these predictions. The chapter will begin with a look into the circular shape derivation, followed by the rectangular shape derivation.

2.1 Circular Shape Theory

Five assumptions were made in order to perform the derivations for the circular shape. (1) The material is homogeneous, meaning that the material properties are consistent throughout the entire specimen. (2) The material is elastic, implying Hooke's Law applies to the specimens. Hooke's Law relates stress to strain through the modulus of elasticity. In the elastic range stress and strain experience a linear relationship, and the slope of this linear line is the modulus of elasticity. (3) The circular shape remains constant. In other words, the cross-section remained circular throughout the entirety of the test. (4) Plane sections remain plane. This concept is illustrated in Figure 2.1.
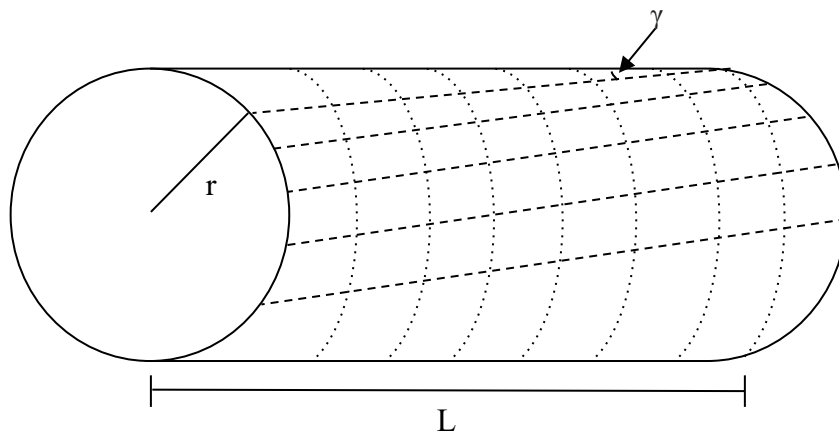
Figure 2.1. Plane sections remain plane.

Notice how all of the smaller pieces depicted in Figure 2.1 move relative to each other. This uniform deformation explains why plane sections remain plane when circular shapes are subject to torque. (5) The final assumption made for the circular shape was that each diameter rotates relative to each other. In more technical terms, the cross-sections rotate as rigid (Ugural, 2018). Using these assumptions, the limits state derivation equations can be derived.

2.1.1 Initial Yielding Derivation

Before yielding, the shear distribution varies linearly with respect to radius, r. Figure 2.2 illustrates this stress distribution.
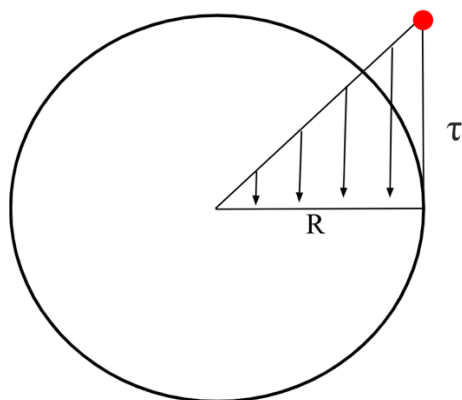
Figure 2.2 Stress distribution before yielding occurs.

The location of the max shear stress, F_{sy}, is illustrated by the red dot at the top of the triangle in

Figure 2.2. This maximum shear stress is dependent on the torque, T, radius, R, and polar moment

of inertia, J. The equation below depicts the relationship between these variables that is used to

find this maximum shear stress:

$$F_{sy} = \frac{TR}{J}$$

The maximum stress is an important value because this stress is when first yield occurs. Because

the maximum shear stress always occurs at the edge of the circle, initial yielding similarly happens

at the outer edge. In order to find the torque value required to create the initial yield, T_y, the

equation listed above can be rearranged to solve for the corresponding torque. The process to find

this value is as follows:

(1) Take the original maximum shear stress equation and solve for T_y.

$$T_y = \frac{F_{sy}J}{R}$$

(2) Substitute the equation for the polar moment of inertia for a circle.

$$T_y = \frac{F_{sy}\frac{\pi R^4}{2}}{R}$$

(3) Simplify the equation, eliminating as many variables as possible.

$$T_y = (0.5\pi)R^3 F_{sy}$$

(4) Write the equation in terms of the diameter of the circle.

$$T_y = (0.5\pi)(\frac{D}{2})^3 F_{sy}$$

(5) Simplify the equation.

$$T_y = 0.196D^3 F_{sy}$$

The equation listed in step 5 presents the initial yield equation for a circular shape in terms of its diameter, D, and shear strength, F_{sy}. It is important to note that the shear strength is 0.6 times the F_{ty} value listed in the aluminum specifications.

2.1.2 Full Yielding Derivation

A specimen will continue to yield until the entire cross-section experiences plastic behavior. Figure 2.3 conceptualizes this idea. The cross-section on the left demonstrates a cross-section that is not yet full yielded, whereas the right cross-section displays a fully yielded cross-section.
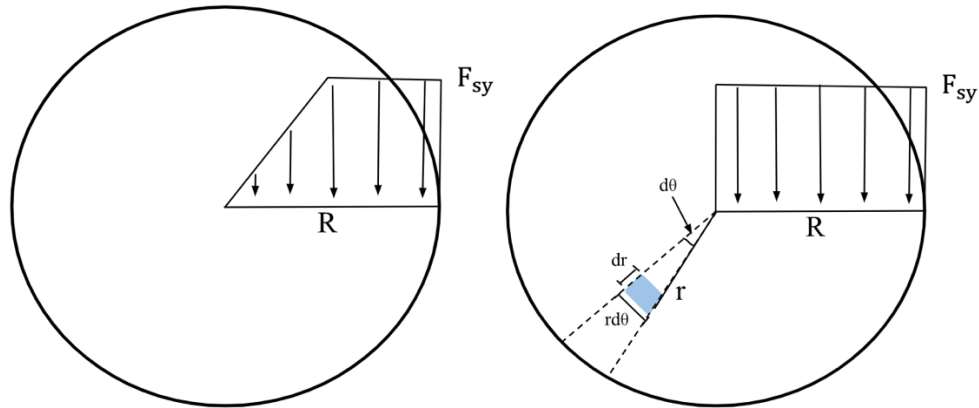
Figure 2.3 Continual yielding and Fully Yielded Cross-section Stress diagrams.

A specimen is fully yielded once the stress distribution is entirely constant, which is illustrated by the horizontal line in Figure 2.3. In order to find the fully yielded torque value, T_p, a double integral in terms of the specimen's radius and rotation angle is required. Torque requires two components, a force and its corresponding moment arm. The derivation to find the equation for torque once a specimen has fully yielded is as follows:

(1) Identify an infinitesimally small piece of the cross-section. The blue piece in Figure 2.3 provides an example of this idea.

(2) Calculate the area, dA, of this piece, assuming a rectangular shape, so the base, r dθ, can be multiplied by the height, dr.

$$dA = r \, d\theta \, dr$$

(3) Find the force, F, over dA.

$$F = dAF_{sy}$$

*Because the specimen is at full yield, the maximum shear stress is applied across the entire cross-section, so F_{sy} is allowed to be used.

(4) Find the applied torque of the infinitesimally small piece from the cross-section.

$$dT = r \, F_{sy}dA = r^2 \, F_{sy} \, d\theta \, dr$$

(5) Sum all of the dT's over all of the possible dA's. In other words, take the integral with respect to r and θ.

$$T_p = \int_{\theta=0}^{\theta=2\pi} \int_{r=0}^{r=R} F_{sy} \, r^2 \, d\theta \, dr$$

(6) Solve the integral and calculate it in terms of the circular shape's diameter.

$$T_p = 0.262 F_{sy} D^3$$

Step 6 depicts the final equation that solves the plastic yield. This equation was used to predict the fully yielded values for the circular shape of the 6061-T6 series.

2.1.3 Rupture Derivation

The rupture derivation is identical to the full yielded derivation except that the ultimate shear strength value, F_{su}, is used instead of the maximum shear strength values. So, the equation used to predict the rupture values was the following:

$$T_P = 0.262 F_{su} D^3$$

2.2 Rectangular Shape Theory

The rectangular shape theory follows a similar procedure; however, more complex math is required to complete these derivations. Ugural and Fenster's fifth Edition of *Advanced Mechanics of Materials and Applied Elasticity* displays relevant theory that helps derive the solid rectangular shape equations. To avoid redundancy and confusion, these derivations will not be included in the report, but the relevant pages from Ugural and Fenster's book can be found in the Appendix (Ugural, Fenster - 2011). Using the same concepts outlined in section 2.1, the derived equations found were as listed below:

$$T_y = \frac{8}{3\alpha} ab^2 F_{sy}$$

$$T_p = 4b^3 \left(\frac{a}{b} - \frac{1}{3}\right) F_{sy}$$

$$T_p = 4b^3 \left(\frac{a}{b} - \frac{1}{3}\right) F_{su}$$

$$\text{Where, } \alpha = 1 + 0.6095\frac{b}{a} + 0.8865 \left(\frac{b}{a}\right)^2 - 1.8023 \left(\frac{b}{a}\right)^3 + 0.91 \left(\frac{b}{a}\right)^4$$

and

Rectangular Bars (a ≥ b):
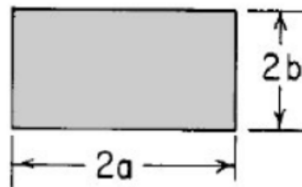
Similar to the circular shape derivation, the fully yielded and rupture equations are exactly the same with the only difference being that the fully yielded equation uses the yield strength, and the rupture equation uses the ultimate strength. Additionally, the variables, a and b can be derived

using the diagram labelled above. Note that in order to find these variables, the width and thickness will need to be divided by two.

One additional note about the yielding of the rectangular shape is that initial yielding occurs at the edge of the shape with the smaller perpendicular distance to the center of the cross-sections. For example, initial yielding would occur on the edge labelled "2a" depicted in the cross-section of the limit state equations presented above.

CHAPTER 3: EXPERIMENTAL RESULTS

Practice trials, calibration measures, and a thorough literature review of the American Society for Testing and Material (ASTM) standards were completed before data collection could begin. After reviewing the applicable ASTM standards for torsion and tension testing, a step-by-step procedure mapping each test's operation practices was created (ASTM E28.04, ASTM E143.20, ASTM A938.18). These outlines ensured accuracy, consistency, and reliability. This chapter will summarize the overall guidelines followed for each test. The actual procedures completed during testing can be found in the Appendix.

The 6061-T6 circular shape was the first cross-section tested, followed by the 6061-T6 and 5052-H32 square shapes. Rectangular shape torsion tests continued by testing them in their ascending aspect ratio order (i.e 2,3,4). Six specimens were tested for each of the desired alloy and cross-section combinations, reaching a total of fifty-four torsion tests. Once the torsion tests were complete, three tension tests were completed to obtain the actual strengths properties of the 6061-T6 and 5052-H32 alloys that were tested in the lab.

This chapter begins with tension testing because the results of these tests were needed to finalize the torsion test results. The report will then present the findings from the torsion testing. Each section starts with a brief introduction, followed by an explanation of the procedure. Lastly, the results of each test are presented. These results are split into two sections: one for each of the aluminum alloys tested on in this study.

3.1 Tension Testing Results

    3.1.1 Introduction

Three tension tests were conducted for each aluminum alloy. The square tension specimens were created using excess aluminum material from the 6061-T6 and 5052-H32 alloys. These specimens were 0.5 in. by 0.5 in. From these tests, the material's true strength values were computed. The 0.2% offset method determined the alloy's yield strength. BlueHill Universal, the software used during tension testing, records an ultimate strength value, so this value was used to report a specimen's ultimate strength.

The 0.2% offset method calculates the yield strength by finding the intersection between the tension test data and a 0.2% offset line that runs parallel to the elastic range (i.e. the linear portion) of the plot. An example of this intersection is depicted in Figure 3.1 by the red dot. The solid line represents the tension data, and the dashed line portrays the 0.2% offset. The stress value at which these two lines interact would be the yield strength of the material. Another name for the slopes of these two lines is the elastic modulus.
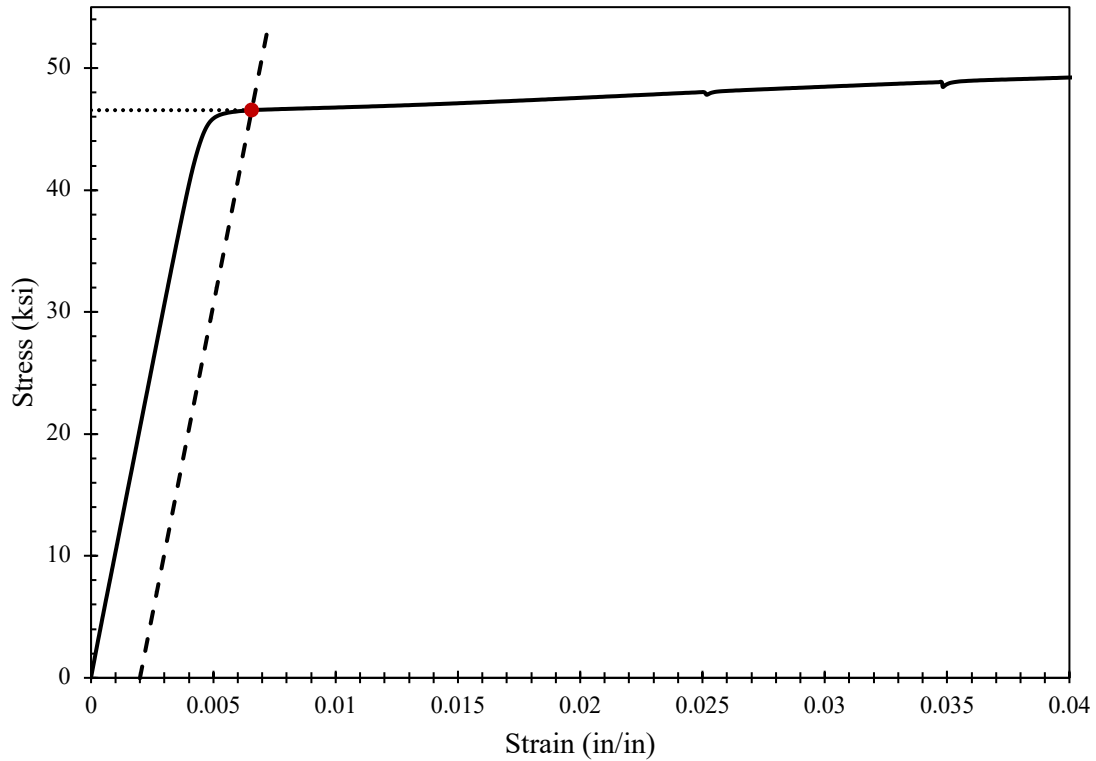
Figure 3.1 Example of 0.2% offset method plot.

To obtain the tension test's corresponding elastic modulus, MS Excel's linear line-of-best fit tool generated a line between data points. For the 6061-T6 alloy, the values of stress used to estimate the slope of the elastic portion ranged between 10-25 ksi. For the 5052-H32 alloy these stress values varied between 4-12 ksi. The ranges were different depending on the alloy because the materials have different strength values. Figure 3.2 provides an example plot for determining the slope value.
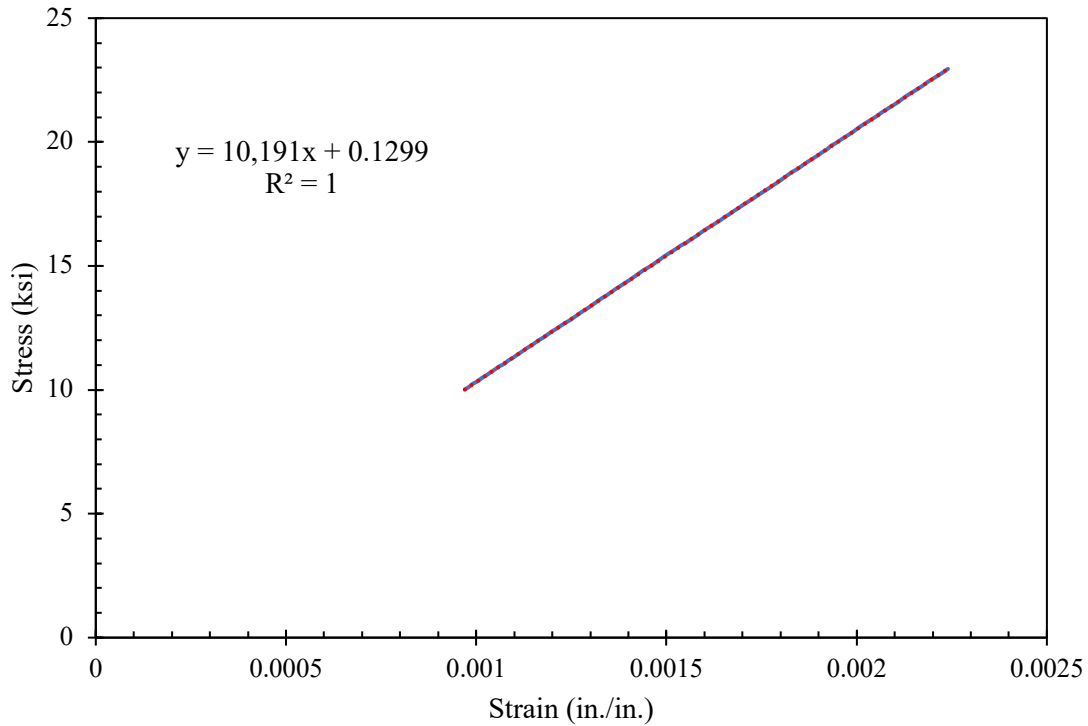
Figure 3.2 6061-T6 Tensile Test 2 Modulus of Elasticity determination plot.

The trendline equation and corresponding coefficient of determination (R^2), which are illustrated in Figure 3.2, are the two crucial pieces of information to take from the plot. The coefficient of determination provides a confidence level for how well the trendline predicts the data. For all of the tension tests, a coefficient of determination equal to one was computed, suggesting that the trendline perfectly predicts the data. As previously stated, the slope of the trendline equation is the modulus of elasticity and was the value used to generate the 0.2% offset line. The equation below demonstrates the general format utilized to obtain the 0.2% offset line:

$$y = E * (x + 0.002) - E * 0.002$$

The variable E corresponds to the slope of the trendline generated from Excel. For example, 10,191 ksi would be the value taken from Figure 3.2. x represents the strain value, and y equals the 0.2% offset stress. Three yield strength and three ultimate strength values were computed for each alloy. These values were later averaged to compute singular strength values for each alloy.

The results will be presented in tabular and graphic form. F_y corresponds to the yield strength, F_u, is symbol for the ultimate strength, and E, represents the modulus of elasticity. Statistical analyses were also conducted on the results and will be presented in this section.

3.1.2 Procedure

The contents of this section outline the tension testing procedure. A full breakdown of this process can be found in the Appendix. Tension tests were completed in accordance with ASTM's *Standard Test Methods for Tension of Metallic Materials* (ASTM E28.04). Three tension specimens for each alloy were prepared using excess material. The sheet-type standard specimen dimension was followed. Key measurements include a gauge width and thickness of 0.5 in., grip section length of 2 in., grip section width of 0.75 in, grip section thickness of 0.25 in., and an overall specimen length of 12.5 in. Section 7.7.1 outlines the offset method employed to find the specimen's yield strength. Testing occurred at a speed of 0.2 in./min, which satisfies Section 7.6.4 requirement that any speed less than the minimum of "one half the specified minimum yield strength or up to one quarter of the minimum tensile strength" can be administered (ASTM E28.04).

Tension Machine

The Instron 5584 testing machine located in the Civil and Environmental Engineering Materials Lab performed the six tension tests conducted for this study. Figure 3.3 provides a full-frontal image of this machine.

Figure 3.3 Tension testing machine.

The compatible software, BlueHill Universal, collected data using an extensometer that was set to one inch. The extensometer measured data until the specimen reached eight percent elongation. Testing quickly halted to remove the extensometer then continued again until rupture. The tension specimen was placed into the grips so that the 0.5 in grip section thickness was visible and not touching the sides of the grips. Figure 3.4 illustrates this specimen and extensometer setup.

Figure 3.4 Tension specimen and extensometer arrangement.

Data Collection

Bluehill Universal converted the data to generate an MS Excel file containing the raw data, a pdf including a displacement (in) vs. Force (lbf) plot, a preliminary 0.2% offset prediction, and the ultimate strength of the specimen. Figure 3.5 and Figure 3.6 demonstrate the kind of plots that BlueHill Universal creates during testing. There is one example for each alloy. A live model of the plot is visible on the monitor during testing.
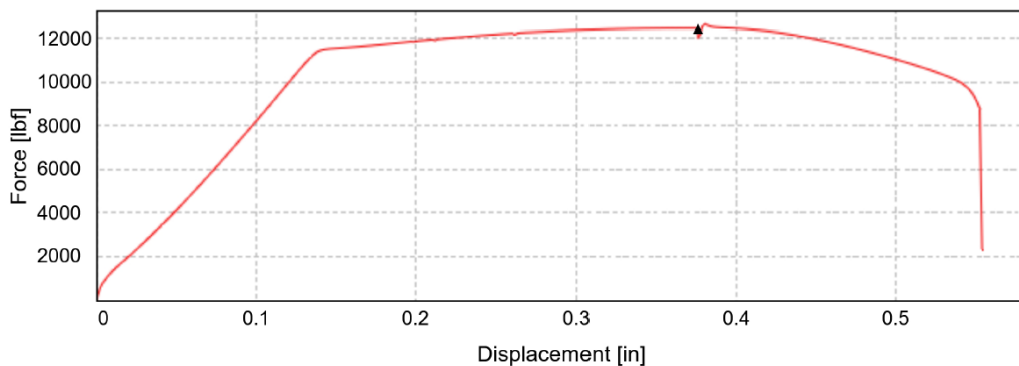
Figure 3.5 6061-T6 raw tension data and plot.
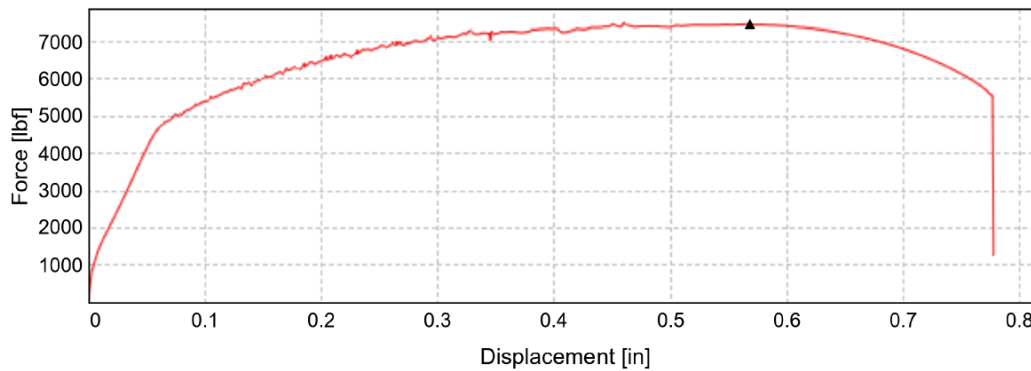
Figure 3.6 5052-H32 raw tension data and plot.

The black triangle found on each plot illustrates the displacement and applied force at the time the extensometer was removed. Figure 3.5 has a slight drop in the data around this triangle. This dip is a direct result of the temporary pausing of the test that occurs to remove the extensometer. The drop is not as obvious in Figure 3.6, rather the noticeable trend in Figure 3.6 is the variability in the inelastic range. This strain hardening section is not smooth as in Figure 3.5. The 5052-H32 alloy is more difficult to grip than the 6061-T6 because of the 5052-H32 alloy composition. This alloy composition has a shiny finish, so during the inelastic range of testing, the grips' restraint on the 5052-H32 alloy likely lost some clutch, leading to the irregularities depicted in Figure 3.7. The red vertical line at the end of each test signifies rupture occurred.

Just as testing begins, the grips need to secure the test specimen into place. This process is depicted at the beginning of each plot and explains the irregularity in the slope that is also illustrated at the beginning of each plot.

The MS Excel files generated from BlueHill Universal were used to apply the 0.2% off-set method on the raw data and find the corresponding yield strengths. Data manipulation was required to convert the raw data to stress values. The force data was divided by the cross-sectional area, 0.25 in^2. The excel file outputted by BlueHill Universal contained a column of strain values that was used to plot the data. Additionally, the pdf that the software outputted contained an estimated yield strength value. Rather than assuming this value to be the yield strength, this number was used as a check to see if the yield strength discovered through the 0.2% offset method seemed reasonable.

3.1.3 Results

3.1.3.1 6061-T6 Tension Results

This section displays the results of the three 6061-T6 tension tests. The findings of these tests are plotted in Figure 3.7 and summarized in Table 3.1.
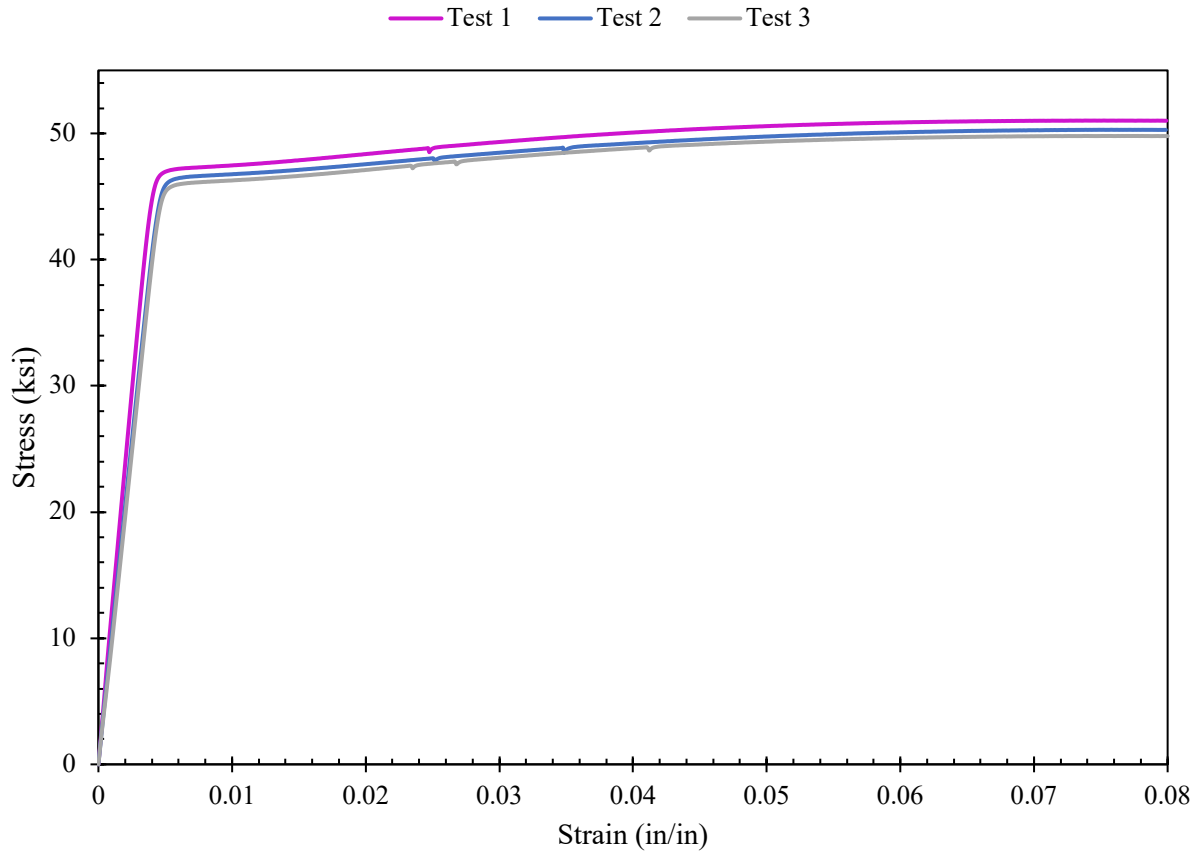
Figure 3.7 6061-T6 Aluminum Tensile Test Results.

The first divot for each of the tests in Figure 3.7 illustrate pauses in the test that occurred while the extensometer was removed from the tensile specimen. Other dips in the plot could be a result of slippage.

Table 3.1 6061-T6 strength values and elastic modulus.

	Test 1	Test 2	Test 3
F_y (ksi)	47.21	46.55	46.05
F_u (ksi)	51.01	50.28	49.79
E (ksi)	11619	10191	10074

Test 1 produced the highest strength values and elastic modulus. The other two tests produced

values with slightly smaller strength values than determined in Test 1.

The results from these three tension tests were compiled and statistically analyzed to find the mean,

standard deviation, and median for the yield strength, ultimate strength, and elastic modulus.

Additionally, confidence intervals were generated around the mean yield and ultimate strength.

The findings from these analyses are summarized in Table 3.2 and Table 3.3.

Table 3.2 Findings of 6061-T6 statistical analysis study.

	Mean	Std.	Median
F_y (ksi)	46.60	0.58	46.55
F_u (ksi)	50.36	0.61	50.28
E (ksi)	10,628	860.2	10,191

Table 3.3 Confidence Intervals for 6061-T6 strength predictions.

	Lower	Upper
F_y (ksi)	45.16	48.04
F_u (ksi)	48.84	51.89

The confidence intervals were created with 95% confidence. Therefore, these ranges imply that

we are 95% confident that the mean strength values for the 6061-T6 material used for this research

fall within the lower and upper limits listed in Table 3.3. Excel's CONFIDENCE.T function output

the confidence value that is added and subtracted to the mean. Assuming a t distribution, this value calculates the interval that is added and subtracted to the mean. Inputted values to this function include the sample size, standard deviation, and confidence level. Both strength confidence interval calculations included a sample size of three and an alpha value of 0.05. The confidence value for the yield strength was ±1.44 ksi and ±1.53 ksi for the ultimate strength.

3.1.3.2 5052-H32 Tension Results

The contents of this section display the results of the 5052-H32 tension tests. The setup is identical to 3.3.2. Figure 3.8 plots the results of these tests.
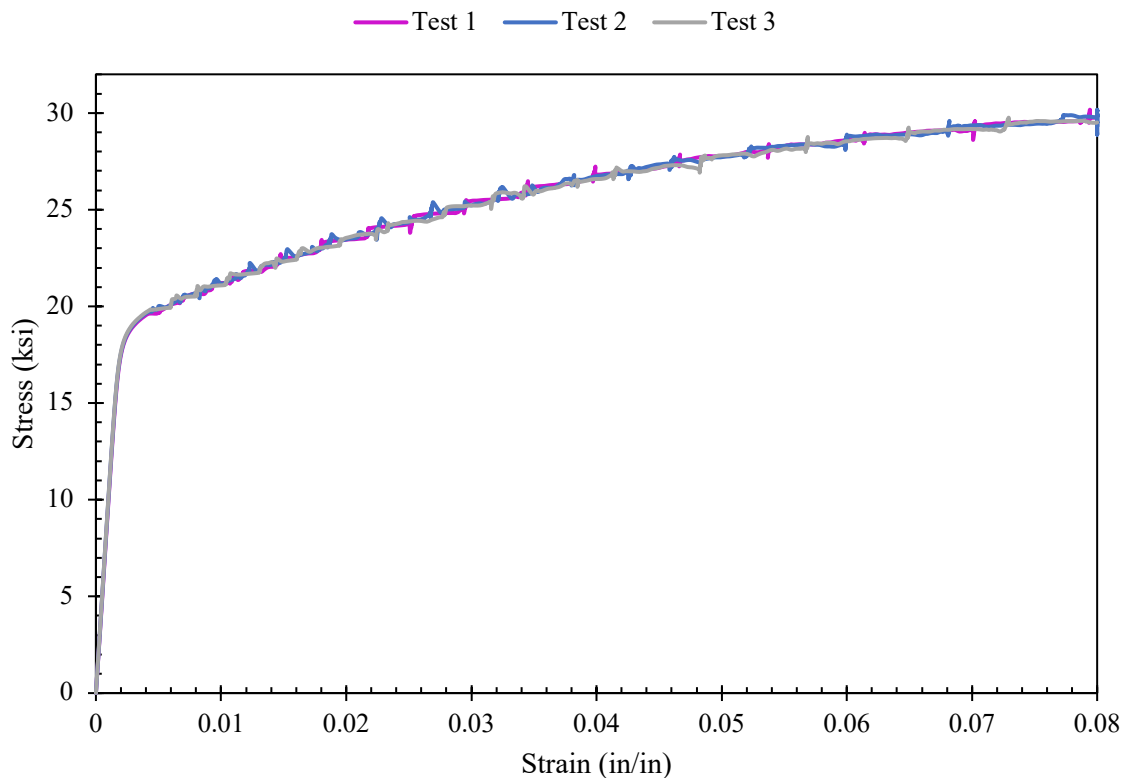
Figure 3.8 5052-H32 Tensile Test Results.

Unlike the 6061-T6 tension tests, the inelastic portion of the 5052-H32 plot does not look as smooth. There are several divots in the inelastic range of each test, which may be a result of the fact that 5052-H32 slips more easily. The elastic range is linear, which suggests that the elastic ranges were unaffected, produced reliable results, and can be used to predict the material's torsional behavior. Table 3.4 presents the calculated strength values and modulus of elasticity for the 5052-H32 series in tabular form.

Table 3.4 5052-H32 strength values and elastic modulus measurements for each test.

	Test 1	Test 2	Test 3
F_y (ksi)	19.52	19.60	19.67
F_u (ksi)	30.39	30.39	30.47
E (ksi)	10,024	10,118	10,072

The results of these tension tests are very consistent. In fact, the ultimate strengths for Test 1 and Test 2 are identical. Further statistical analysis was performed on the results of tension tests. Table 3.5 summarizes the findings.

Table 3.5 5052-H32 statistical analysis findings.

	Mean	Std.	Median
F_y (ksi)	19.60	0.07	19.60
F_u (ksi)	30.42	0.05	30.39
E (ksi)	10,071	47	10,072

Further analysis performed on the mean strength values generated confidence intervals. These ranges are listed in Table 3.6.

Table 3.6 Confidence Intervals for 5052-H32 strength predictions.

	Lower	Upper
F_y (ksi)	19.42	19.78
F_u (ksi)	30.29	30.54

An alpha value of 0.05 conducted the test. In other words, Table 3.6 provides 95% confidence intervals. Excel's CONFIDENCE.T function output the confidence value that is added and subtracted to the mean. For the yield strength, this value was ± 0.18 ksi and ± 0.13 ksi for the ultimate strength.

3.2 Torsion Testing Results

3.2.1 Introduction

The purpose of this section is to present the results obtained through torsion testing so that discussions and conclusions related to the topic of this report can be addressed. This section will begin by explaining the torsion testing procedure and describe the equipment and software used to collect data. Then, the report will introduce the calibration procedure that was created to generate reliable data. Finally, the experimental results will be presented with the 6061-T6 torsion results displayed first and will then be followed by the results of the 5052-H32 torsion tests.

The specimens tested include circular rods and square and rectangular bars. The circular rods were only tested for the 6061-T6 series and have a diameter of 0.75 in. The bars all had a thickness of 0.5 in. with varying widths of either 0.5 in, 1.0 in, 1.5 in, or 2.0 in. Each bar shape was tested for

both alloys. When reporting the results of the bar shape torsion results, the corresponding aspect ratios will differentiate them. An aspect ratio is determined by dividing the height of the specimen from its width. For instance, the 1.0 in by 0.5 shape will be labeled as "w/h = 2."

3.2.2 Procedure

The full torsion testing procedure can be found in the appendix. This section will simply provide a brief summary of the procedure and equipment used for testing so that a general understanding of the testing process is obtained.

There are currently no ASTM standards related to torque testing of circular or rectangular shaped cross-sections, so the testing protocol followed ASTM A938*: Torsional Testing of Wire* (ASTM A938-18). The important takeaways from this standard that apply to this study include the specimen preparation and the procedure sections. Initial yield occurs on the outer edge of the aluminum alloy because the testing specimen experiences maximum shear stress on the surface. As a result, the standard emphasizes the importance of maintaining a smooth surface. Even the slightest indentation could lead to inaccurate results because an impression would create an early fracture. The specimen would begin yielding at a smaller torque value than anticipated. The procedure section recommends that testing occur at a maximum speed of 30 degrees/min for wires with diameters of 0.142 in. or larger (ASTM A938-18). This maximum speed was used once the inclinometers were removed from the testing specimen and all of the yielding data needed for this study had been collected. The torsion machine operated on the lowest setting while collecting yielding data so that the most amount of data could be collected. The machine then switched to thirty degrees per minute while determining the experimental rupture values. The increase in speed

was to reduce the total testing time for each specimen. Applying this method, a single test took approximately one hour.

Torsion Machine

The torsion machine located in the Civil and Environmental Engineering materials lab conducted all of the torsion tests. Figure 3.9 illustrates a frontal image of this machine.

Figure 3.9 Torsion Machine that was used to run experiments.

The testing specimen is placed between the two red cylinders pictured in Figure 3.9. The red cylinders twist the specimen and include the grips that hold the specimen in place. The left grip holds the specimen in the original starting position, while the right grip twists the specimen. The grips used to run a test depended on the cross-section of the specimen. The five grip orientations used for testing are illustrated in Figure 3.10.
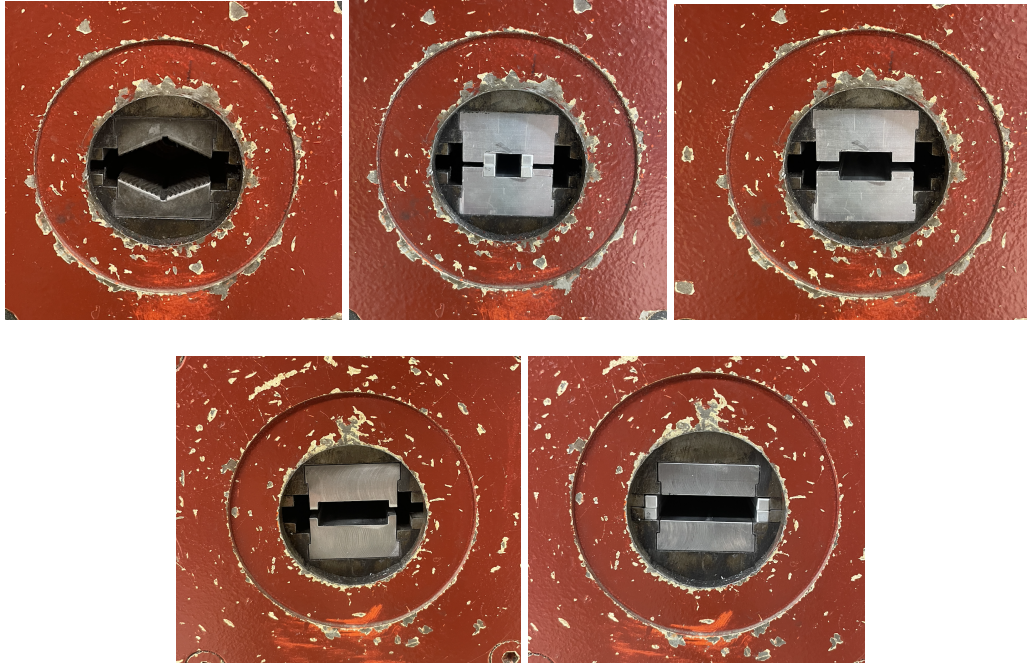
Figure 3.10 Grips used for torsion testing.

The grips were constructed using 6061-T6 aluminum. The square shape and w/t = 4 shape grips required four aluminum fillers to be placed in the grips in order to fit the test specimen into the grips. Two of these aluminum fillers were stacked on each side of the grip. This design is illustrated in Figure 3.10. The purpose of these fillers was to secure the test specimen in place. Interestingly, the grips for the square shape and the w/t = 2 shape used the same grips; however, inserting the aluminum fillers into the grips creates the square shape desired for testing.

Tests ran in the same direction at the same speed. The only varying machine component was the scale that conducted the tests. The possible scales include 1,200 in-lb., 6,000 in-lb., 24,000 in-lb., and 60,000 in-lb. Only two scales, 1,200 in-lb. and 6,000 in-lb., collected torque data. For the w/t = 4 shape the machine was switched to the 24,000 in-lb. scale after inclinometer data collection

stopped and the devices were removed in order to find the rupture values. Figure 3.11 displays the dial that converts the scale that administers the test.
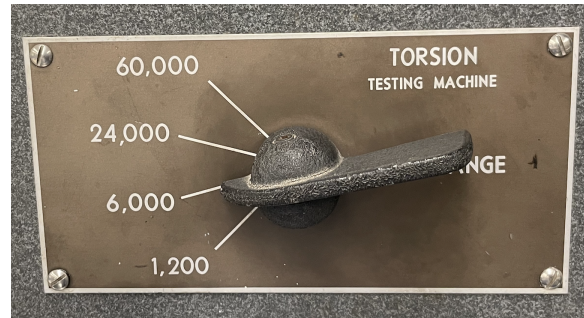
Figure 3.11 Dial used to change torque range during testing.

The specimen was prepared following the same procedure for each test. First, the aluminum specimen was inserted into the right grip. Then, the orange wheel was spun until the left side of the torsion machine was closer to the specimen. This dial, which is illustrated in Figure 3.11, was spun until an 11.5 in. pvc spacer touched both red cylinders. Once the specimen was loosely secure in the machine, the methods to zero the machine could commence. To start, the right grip was tightened to capacity. This action would often induce inaccurate torsion readings on the machine, so the torque reader was manually set back to zero using the appropriate knob as depicted in Figure 3.12.

Figure 3.12 Knobs that zero the torsion machine.

Once the machine was zeroed, the left grip is tightened to capacity. Again, this process generates small torque readings. However, these torque values are accurate because the specimen was secured by both grips. Therefore, the machine was used to zero itself by running the machine in the opposite twisting direction (i.e. clockwise). Pushing the green button twisted the specimen in the desired direction. Once the torque reader reached zero, the red "stop" button was pushed. The buttons that operate these mechanics are displayed in Figure 3.13.

Figure 3.13 Buttons that begin and end testing.

Inclinometers

Data was collected using WitMotion Bluetooth 2.0 Inclinometers and their compatible software package. For the purposes of this report, the device will be referred to as an inclinometer. Figure 3.14 presents a plan view of one device and illustrates the directions of the X, Y, and Z axes. The inclinometer's bluetooth capabilities, three axis orientation, and timely data collection patterns not

only enhanced the precision of the torsion test, but also, the device eliminated human error. Before the inclinometers were discovered, torque and phi values were manually recorded by the people operating the machine. Historically, one individual would read a torque value, and the other individual would read the corresponding angle of twist value. Hypothetically, these values were recorded at the exact same time. However, this dated testing method results in unreliable and significantly less data collection, as humans cannot collect data down to the milliseconds.

Figure 3.14 Plan and side view of inclinometer.

Three inclinometers operated while compiling data: two attached to the specimen and one mounted to the back of the torsion machine on a gear that moved relative to the applied torque. The two inclinometers sitting on the aluminum alloy had a small "L" bracket attached to the bottom of the device, as illustrated in Figure 3.14, so that the inclinometer could be attached to the specimen in the same plane each test. The devices were separated by a standard 7.13 in. each test. To achieve the 7.13 in. of space between the devices, an unused tension specimen was placed between them. The tension specimen acted as a spacer. The tension specimen was 7.0 in, however, to find the actual distance between the inclinometers, a $\frac{GJ}{L}$ study was conducted, and the equation was rearranged to solve for L. More information about this study will be discussed in Chapter 3. The left inclinometer would be taped to the aluminum specimen. Then, the spacer would be placed on

the testing specimen so that the spacer was touching the right edge of the inclinometer Next, the right inclinometer would be taped to the test specimen. The right inclinometer needed to touch the exposed edge of the spacer while the inclinometer was being taped to the test specimen. Figure 3.15 illustrates this idea.
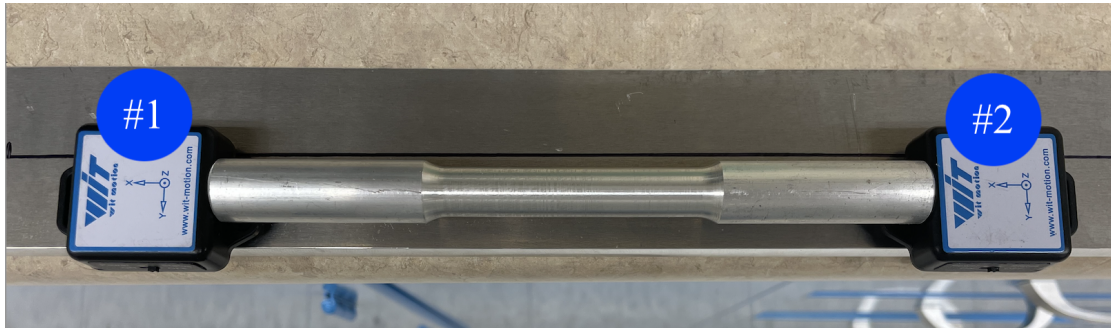
Figure 3.15 Inclinometer setup spaced by the tension specimen.

The data from these two inclinometers was used to determine the Phi value. Phi was determined by subtracting the x-axis angle results of inclinometer #1 from the x-axis results of inclinometer #2. The specimen was always twisted so that inclinometer #2 rotated more than inclinometer #1. As a result, the difference was always positive.

The third inclinometer that was taped to a gear on the back of the torsion machine remained fixed to the machine throughout the duration of this study. This inclinometer's data determined the applied torque on the specimen. The process to achieve the relationship between the applied torque and the inclinometer's rotation will be described in 3.2 Calibration Results. It was essential that the third inclinometer remain fixed to the machine throughout testing so that this relationship remained constant. Figure 3.16 depicts the location of the third inclinometer.
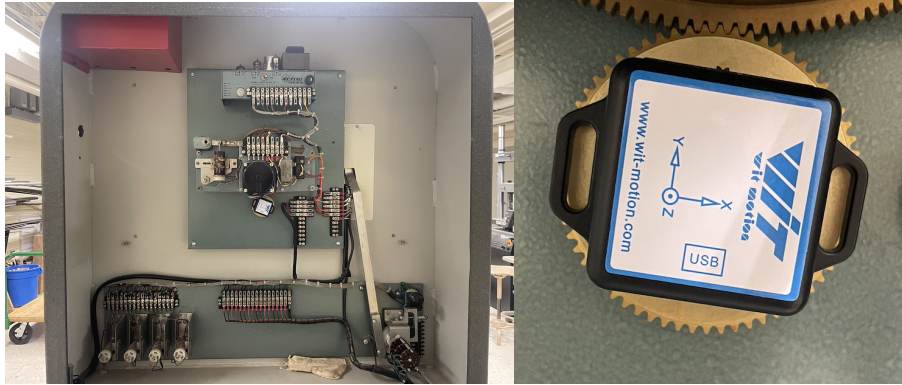
Figure 3.16 Inclinometer taped to the back of the torsion machine.

Data Collection

WitMotion's compatible software program, MiniMu, collected the data from the three inclinometers and stored it into a text file. MiniMu operated three different browsers at once, relating one browser to each inclinometer. The browser configuration presented in Figure 3.17 demonstrates the setup applied during testing.
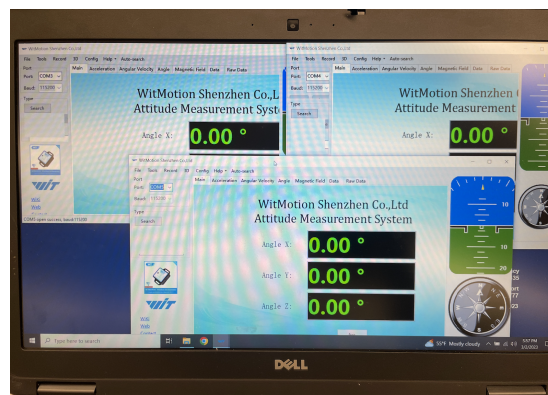
Figure 3.17 Computer face during data collection.

The top right browser connects to inclinometer #2, the left to #1, and the bottom browser to the inclinometer on the back of the machine. The angle data in the x direction is of interest for the two

inclinometers on the test specimen, whereas the inclinometer on the back of the machine relies on the y-axis angle data.

Before testing began, all of the inclinometers needed to be zeroed. Once the devices matched the screen depicted in Figure 3.18 testing and data collection could begin. Data collection occurred until the difference between the two angles in the top browsers read greater than 90 degrees, meaning that the two inclinometers on the on the test specimen had been rotated at least 90 degrees relative to each other. Then, the data was imported into an MS Excel spreadsheet and adjusted to generate the relationship between phi and torque.

Data Conversion

In order to convert the data collected from the inclinometers to corresponding torque values, a series of steps had to be completed. The inclinometers only output data degree values between a certain range. This range depends on the axis of interest. For example, the x-degree values range between -180 and +180 degrees, whereas the y-degree values vary from -90 to 90 degrees. Once a device reached one of the limits and continued to move in the same direction, the inclinometer would begin to output values in the opposite direction. For instance, if the inclinometer reached -90 degrees in the y-direction, the next output value if the same motion continued, would be -89 degrees. The same holds true for the positive direction. If 90 degrees is reached in the y-direction and the device moves in the same direction, then the next number outputted would be 89 degrees. It is important to note that these conditions hold true for this research because the direction of movement remained constant, meaning several axes were constant.

The measured angles needed to be continuous, meaning the phi values needed to continually increase. Fortunately, the two inclinometers on the testing specimen never hit a limit, so no data manipulation was required. However, the inclinometer on the back of the machine rotated a full 360 degrees several times. Therefore, data manipulation was necessary. The equation below provides the general format utilized to obtain the degree values:

$$Y_{i+1} = Y_i + ABS(X_2 - X_1)$$

The Y values represent the new angle values, while the X values correspond to the degree values computed by the inclinometer. Essentially, the absolute difference between the two actual degree values is added to the previous degree value. With these new degree values, a corresponding torque can be calculated.

Converting these new degree values to a corresponding torque value required further data manipulation. The angle transformed into a torque value through the FORECAST function in MS Excel. This function interpolates data through linear regression to predict a value. In terms of this research, the FORECAST function performed interpolation on calibration data collected on the 1200 in-lb and 6000 in-lb scales. The calibration data for each scale is presented in Table 3.7 and Table 3.8.

Table 3.7 1200 in-lb. calibration raw data.

Av. Angle (degrees)	Torque (in-lb.)
0	0
81.88	100
163.73	200
240.30	300
308.30	400
385.31	500
465.01	600
551.68	700
622.99	800
690.86	900
768.52	1000
857.00	1100
940.69	1200

Table 3.8 6000 in-lb. calibration raw data.

Angle (degree)	Torque (in-lb.)
0	0
103.74	600
203.92	1200
284.96	1800
370.05	2400
474.24	3000
571.20	3600
651.17	4200
735.96	4800
841.79	5400
949.21	6000

Section 3.2.3 describes how this raw data was collected and converted to a calibration dataset in more detail.

3.2.3 Machine Calibration

The torque values generated through data analysis depended heavily on the calibration results. Therefore, this data needed to be as accurate as possible. Calibration data was briefly collected before torsion testing began so that preliminary data manipulation could start. However, the torsion data was later updated using the more reliable calibration data through a process that will be outlined in this section.

To achieve this precision, two NEIKO torque adapters were purchased and used on the torsion machine. The torque cells varied in capacity and accuracy. The higher capacity adapter computed torque values ranging from 1,800 in-lb. to 9,000 in-lb., whereas the lower capacity adapter ranged from 176.4 in-lb. to 1,195.2 in-lb. Both devices provided results within two percent accuracy. Figure 3.18 displays an image of the lower capacity adapter. The higher capacity adapter looks identical to the lower capacity adapter, except the dimension are larger.

Figure 3.18 Frontal Image of Torque calibration device.

To collect data, the adapter was inserted into the torsion machine as picture in Figure 3.19. A wrench was attached to the end of the adapter that was not supported by the torsion machine. Thus, only the left grip of the machine was used for testing.
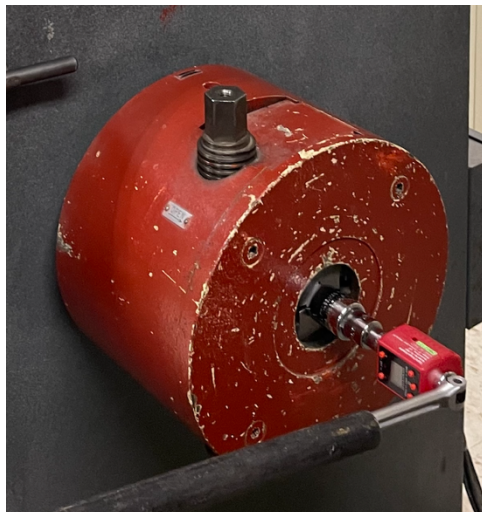
Figure 3.19 Torque adapter testing configuration.

The torque value read off the adapter needed to increase or remain constant. A decrease in the torque reading would cause the inclinometer data to be unreliable. The data manipulation process, as outlined in Section 3.1.2, assumed that the torque readings were either increasing or fixed. Consequently, the wrench attached to the adapter was inserted into a hollow pipe that rested on a lifting table. Twisting the dial on the table moved the wrench so that the torque readings would always increase.

Collecting the calibration data required two individuals. One person operating the lifting table and simultaneously reading the adapter values, while the other person monitored the computer screen

and took photos of key angle values. The individual reading the adapter told the computer operator when to snap the photos. Figure 3.20 depicts an example of a photo taken during testing.
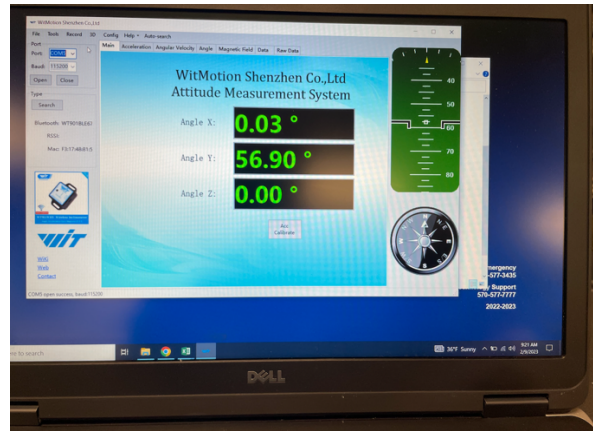
Figure 3.20 Angle measurements to convert to torque value.

The inclinometer on the back of the machine collected data during testing so that the angles could be converted to continuous values using the equation presented in the previous section. Then, using the photos time stamp and comparing it to the time column of the data, torque values were placed with their appropriate gear angle. For the 1200 in-lb. scale, angle values were recorded every 100 in-lb. The 6000 in-lb. scale reported measurements every 600 in-lb. These measurements were then confined to form Table 3.9 and Table 3.10.

Because of the ranges of the adapters varied, four values needed to be removed from the raw data. The first data point removed was the 100 in-lb. torque reading from the 1,200 in-lb. scale because 100 in-lb. is not within the lower capacity adapter's range of reliable torque values. Additionally, the maximum point, which correlated to a 1,200 in-lb. torque value was removed because this measurement was slightly larger than the maximum recordable torque value for the smaller

adapter. For the same reason, two reading needed to be removed from the 6,000 in-lb. scale data: the 600 in-lb. and 1,200 in-lb. readings. The 6,000 in-lb. scale was tested using the higher capacity adapter, so reliable torque readings could not start until 1,800 in-lb.

In order to use the updated calibration data in the torsion excel spreadsheets, the torque values needed to be normalized, meaning the torque values needed to range between zero and one. The values were normalized by dividing the torque values by the scale level used during data collection. For example, the 1,200 in-lb. torque values were divided by 1,200. Table 3.9 and Table 3.10 present these normalized torque values with their corresponding angle measurements for the 1,200 in-lb. and 6,000 in-lb. scale respectively.

Table 3.9 1200 in-lb. normalized calibration data.

Angle (degrees)	Normalized Torque
0	0.00
163.7	0.17
240.3	0.25
308.3	0.33
385.3	0.42
465.0	0.50
551.7	0.58
623.0	0.67
690.9	0.75
768.5	0.83
857.0	0.92

Table 3.10 6000 in-lb. normalized calibration data.

Angle (degrees)	Normalized Torque
0.0	0.00
285.0	0.30
370.1	0.40
474.2	0.50
571.2	0.60
651.2	0.70
736.0	0.80
841.8	0.90
949.2	1.00

To verify that the calibration results were consistent for both scales, the angle measurement were

plotted against the normalized torque values. Figure 3.21 presents the results of this comparison.
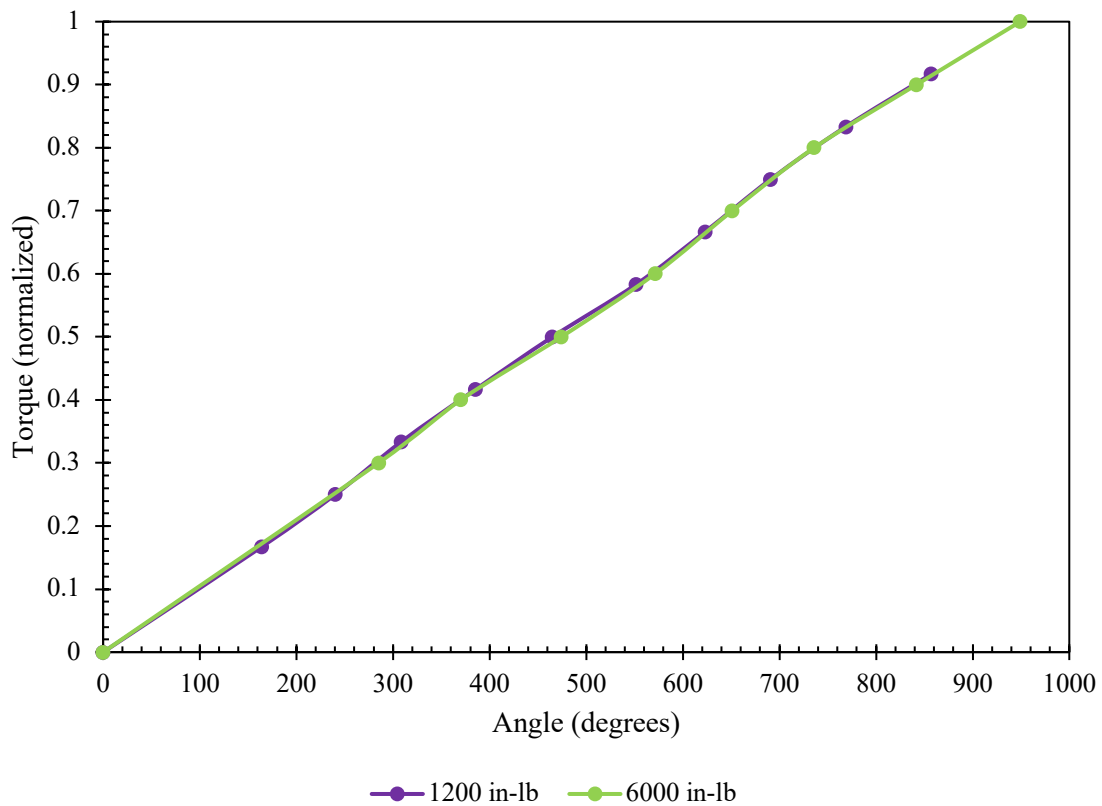
Figure 3.21 Calibration results for the torsion machine.

Figure 3.21 proves that the data sets are nearly identical. The 6,000 in-lb. line falls directly on the 1,200 in-lb. line. This plot confirms that these data sets are reliable and can be used to convert the rotation data into corresponding torque values. Thus, the 1,200 in-lb. calibration data converted angle measurements into torque values when the 1,200 in-lb. scale ran a torsion test, and the same conditions apply for the 6,000 in-lb. calibration data.

3.2.4 6061-T6 Results

The results presented in this section include the findings obtained from the 6061-T6 torsion testing. These results were plotted and compared to the initial yield, full yield, and rupture values computed using the strength values determined from the tension testing and the strength values listed in the *Specifications for Aluminum Structures*. To differentiate between these two methods, any calculations performed with tension test strengths, "Predicted" will follow the description. Likewise, "ADM," the acronym for *Aluminum Design Manual*, will proceed any description where the strength values listed in the *Specification for Aluminum Structures* were used. The initial yield value is 35 ksi, and the ultimate strength listed in the specification is 42 ksi. This concept also applies to the 5052-H32 series.

Both methods calculated the yield and rupture values using the equations presented in Chapter 2. Table 3.11 and Table 3.12 report the final answers of these equations for each method.

Table 3.11 6061-T6 Initial Yield, Full Yield, and Rupture values - Predicted.

	Shape				
	Circular	Square	w/t=2	w/t=3	w/t=4
T_y (in-lb.)	2,316.2	726.5	1,715.9	2,804.8	3,938.8
T_p (in-lb.)	3,088.3	1,165.1	2,912.7	4,660.3	6,407.9
T_u (in-lb.)	3,337.4	1,259.0	3,147.6	5,036.2	6,924.7

The mean strength values discovered through tension testing were the assumed strength properties used to calculate the predicted initial yield, full yield, and rupture limit states calculated in Table 3.11. These values were calculated for each cross-section.

Table 3.12 6061-T6 Yielding and Rupture values - ADM.

	Shape				
	Circular	Square	w/t=2	w/t=3	w/t=4
T_y (in-lb.)	1,739.5	545.6	1,288.7	2,106.5	2,958.1
T_p (in-lb.)	2,319.4	875.0	2,187.5	3,500.0	4,812.5
T_u (in-lb.)	2,783.3	1,050.0	2,625.0	4,200.0	5,775.0

The initial yield, (T_y), and full yield, (T_p), values from both tables will be compared to data collected from the inclinometers, whereas the rupture values, (T_u), will be compared to experimental values recorded from the torsion machine.

3.2.4.1 Initial Yield Results

The plots presented in Figure 2.22 display initial yield values plotted over the experimental torsion data. The solid, black horizontal line corresponds to the initial yield value computed using the predicted yield strength, 46.60 ksi, whereas the dashed line represents the initial yield value obtained using the yield strength listed in the *Specification for Aluminum Structures*, 35 ksi (ADM). To keep the results consistent and avoid the use of outliers, three or four of the tests were plotted for each cross-section.
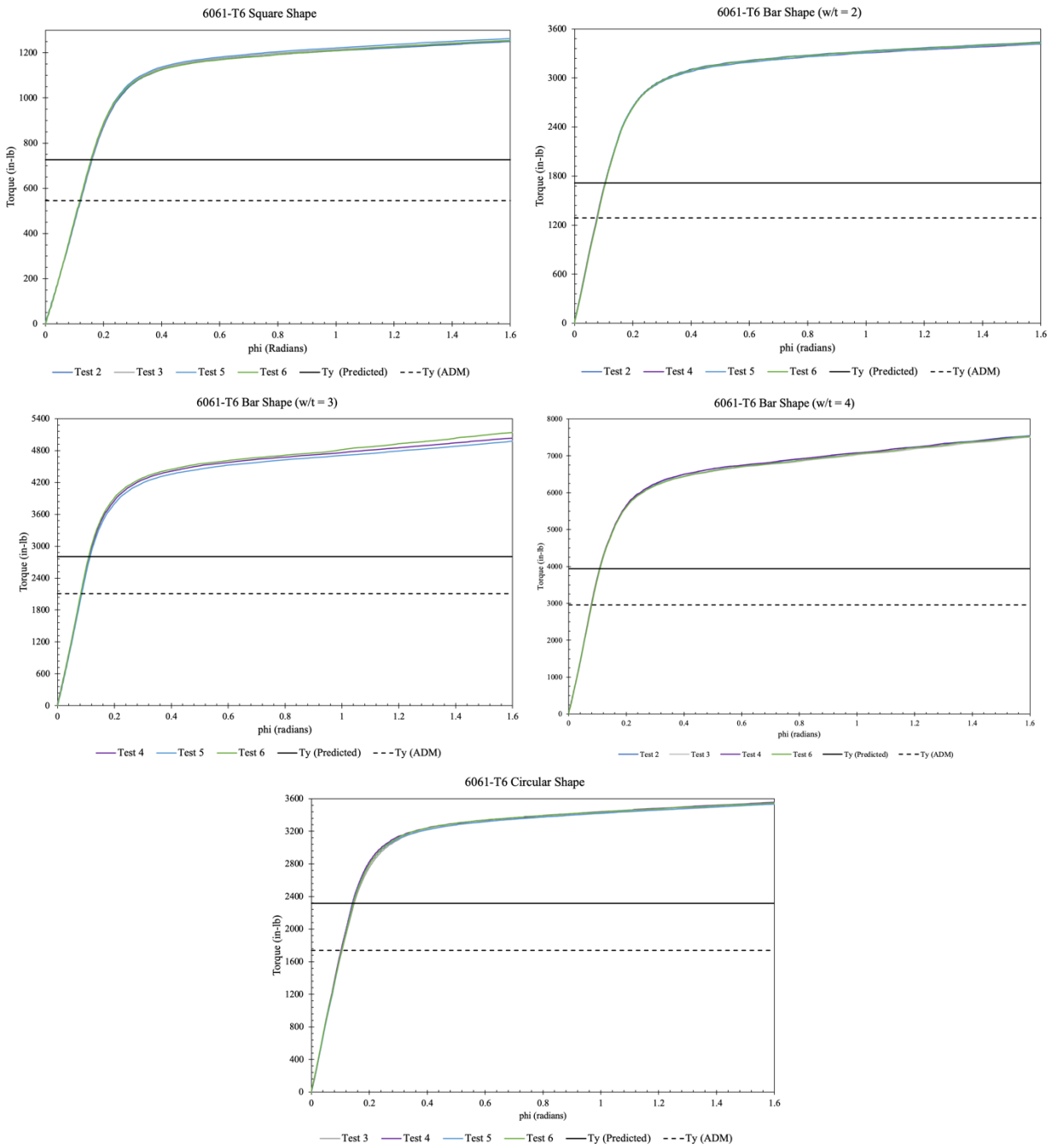
Figure 3.22 6061-T6 Torsional Test results with Initial Yield Predictions.

3.2.4.2 Full Yield Results

The contents of this section display the torsion data with the full yield estimations. This procedure means that the full yield equation presented in Chapter 2 were used for this section. Similar to the previous section, the solid horizontal line correlates to values using a yield strength of 46.6 ksi from tension testing. The dashed horizontal line corresponds to full yield values determined using the 35 ksi yield strength that is listed in the *Specification for Aluminum Structures*. The results are plotted in Figure 3.23.
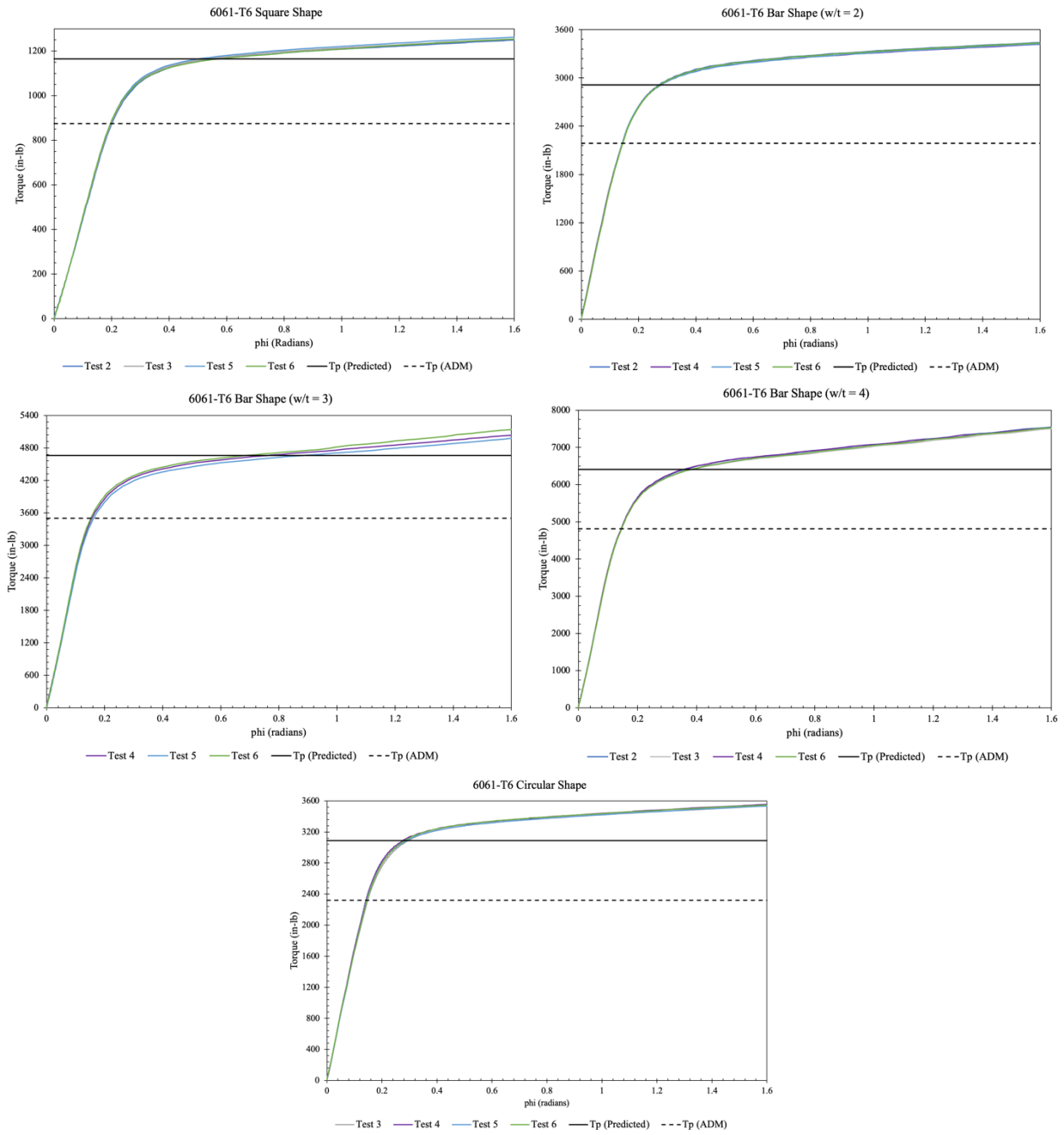
Figure 3.23 6061-T6 Torsion Test results with Fully Yielded Prediction Values.

3.2.4.3 GJ/L Study Results

The results presented in this section include the findings of the $\frac{GJ}{L}$ study that was conducted on the 6061-T6 torsion data. The $\frac{GJ}{L}$ value can be found using the plots to determine the slope of the elastic region, or in other words, the slope of the line until the specimen reaches initial yield. MS Excel's "LINEST" tool calculated these slopes and was then plotted over the torsion data. The $\frac{GJ}{L}$ values for each cross-section can be found in Figure 3.24 and are depicted by the dashed red line. Further data analysis conducted on the torsion data is presented in Table 3.13 and Table 3.14.
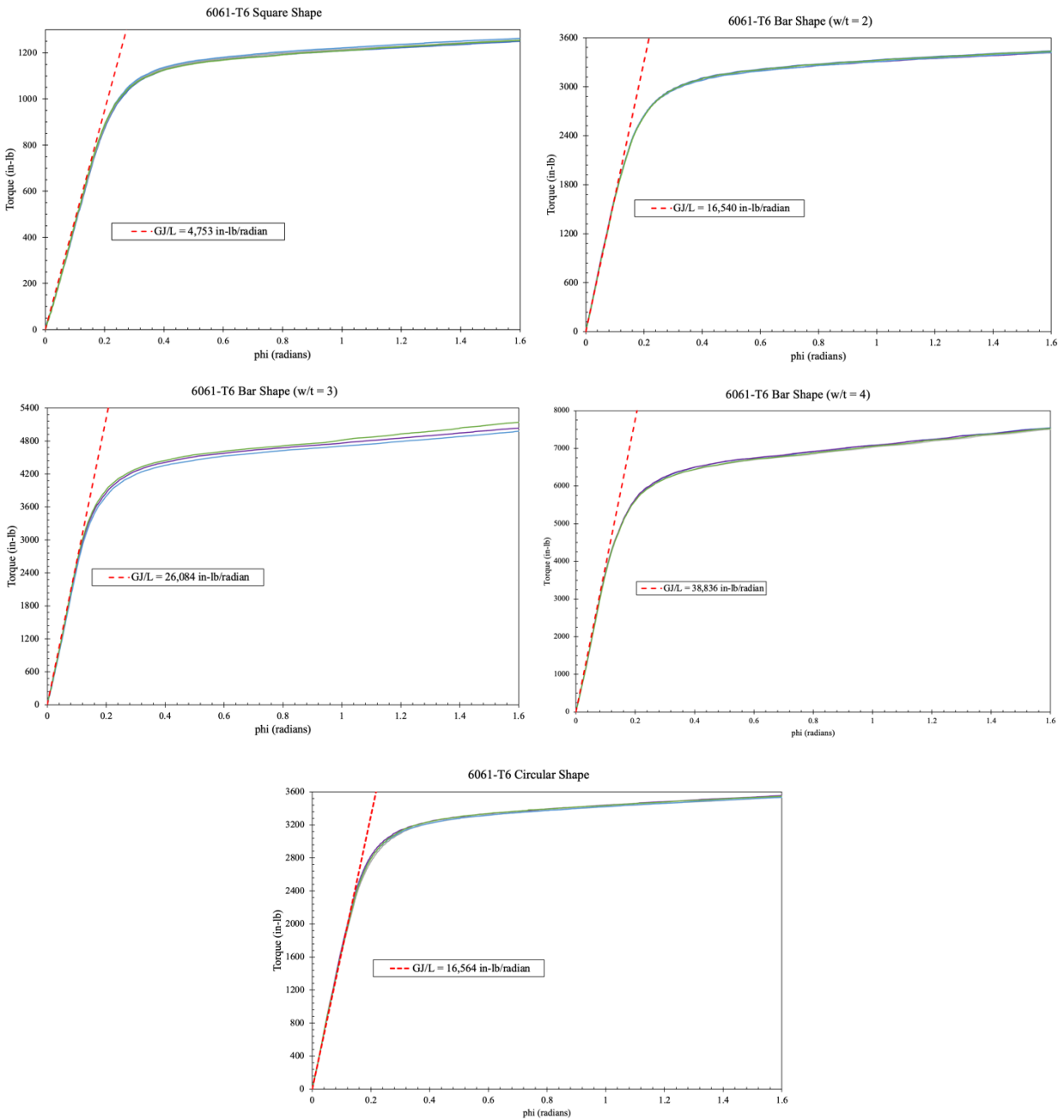
Figure 3.24 6061-T6 $\frac{GJ}{L}$ study results.

Table 3.13 6061-T6 $\frac{GJ}{L}$ values.

	Rod	Square	w/h=2	w/h=3	w/h=4
Predicted (k-in./radians)	16.700	5.041	15.381	26.551	37.747
ADM (k-in./radians)	16.564	4.683	15.256	26.335	37.439
Actual (k-in./radians)	16.564	4.752	16.540	26.084	38.836

Table 3.13 presents the $\frac{GJ}{L}$ values found using three different methods. The Predicted and ADM

values use the median Modulus of Elasticity to find and Shear modulus, G. The polar moment of

inertia equations listed in Budynas and Sadegh's *Roark's formulas for stress and strain* were

used to find the equivalent J values (Budynas, Sadegh- 2020). These polar moment of inertia

equations can be found in the Appendix. Essentially, a specimen's polar moment of inertia is its

resistance to being deformed by torsion. The final component of the ratio, L, was the fixed length

determined through a back calculation using the circular rod data. The expected shear modulus

and polar moment of inertia were multiplied, then the average of the "LINEST" tool results of

the circular rod divided from this product. The values listed in the Actual row are the results of

MS Excel's "LINEST" tool.

Table 3.14 6061-T6 $\frac{GJ}{L}$ ratios.

	Rod	Square	w/h=2	w/h=3	w/h=4
Predicted (k-in./radians)	0.99	0.94	1.08	0.98	1.03
ADM (k-in./radians)	1.00	1.01	1.08	0.99	1.04

The ratios listed in Table 3.14 are a result of dividing the Predicted or ADM from the Actual

row. For example, the 1.02 for the ADM row in the Square column was found by $\frac{4.752}{4.670}$. A ratio of

1.00 indicates that the estimated values match the Actual prediction, and the data is reliable.

3.2.4.4 Rupture Results

The contents of this section outline, present, and compare the 6061-T6 series rupture results. The

experimental rupture results from torsion testing are listed in Table 3.15.

Table 3.15 Experimental rupture values for 6061-T6.

	Test 1	Test 2	Test 3	Test 4	Test 5	Test 6
Circular (in-lb.)	3,640	3,655	3,660	3,655	3,640	3,655
Square (in-lb.)	1,425	1,400	1,405	1,430	1,410	1,400
Bar (w/t=2) (in-lb.)	4,110	4,135	4,100	4,100	4,135	4,155
Bar (w/t=3) (in-lb.)	7,380	7,360	7,370	7,520	7,120	7,120
Bar (w/t=4) (in-lb.)	N/A	11,840	11,880	11,840	12,040	11,940

Rupture results were independent of any inclinometer data, so values collected for tests that were

removed for yielding results were kept in the results table. The data support this action because

the rupture values vary within a reasonable range.

The first test of the bat with an aspect ratio of four has an "N/A" because this test was not run

through rupture. As a result, no rupture value could be recorded.

Statistical analysis procedures were completed on the findings from these experiments. The mean, standard deviation and median values are present in Table 3.16 and 95% confidence intervals about the mean are illustrated in Table 3.17.

Table 3.16 Statistical Analysis Results for 6061-T6 Experimental Rupture Values.

	Mean	Std.	Median
Circular (in-lb.)	3,650.83	8.61	3,652.92
Square (in-lb.)	14,11.67	12.91	1,407.50
Bar (w/t=2) (in-lb.)	4,122.50	22.53	4,116.25
Bar (w/t=3) (in-lb.)	7,311.67	159.55	7,335.83
Bar (w/t=4) (in-lb.)	11,908.00	84.38	11,880.00

Table 3.17 Confidence Intervals for the Mean Experimental Rupture Results.

	Lower	Mean	Upper
Circular (in-lb.)	3,641.80	3,650.83	3,659.87
Square (in-lb.)	1,398.12	1,411.67	1,425.21
Bar (w/t=2) (in-lb.)	4,098.86	4,122.50	4,146.14
Bar (w/t=3) (in-lb.)	7,144.23	7,311.67	7,479.11
Bar (w/t=4) (in-lb.)	11,803.23	11,908.00	12,012.77

The confidence intervals listed in Table 3.17 assume 95% confidence. These ranges suggest that we are 95% confident that the rupture values for various cross-sections using the 6061-T6 material that conducted the torsion tests fall within the limits listed in Table 3.17.

Three different rupture values were recorded for each 6061-T6 cross-section: Two equation-based estimations and one experimental observation. Table 3.18 lists these three different values for each cross-section.

Table 3.18 6061-T6 Rupture Results.

	Circular	Square	w/h=2	w/h=3	w/h=4
Predicted (in-lb.)	3,337.37	1,259.05	3,147.61	5,036.18	6,924.75
ADM (in-lb.)	2,783	1,050	2,625	4,200	5,775
Actual (in-lb.)	3,650.83	1,411.67	4,122.50	7,311.67	11,908.00

Two of these approximations used the rupture equations presented in Chapter 2. The only difference between these two values that is the ultimate strength, F_u, inserted into the equation. The Predicted approximations use an ultimate strength of 50.36 ksi, which is the mean ultimate strength discovered through tension testing. The ADM estimations follow the ultimate strength provided in the *Specifications for Aluminum Structures*, which is 42 ksi. The large gap between these two ultimate strength values explains the disparity among two rows. The row labeled "Actual" lists the mean rupture value computed for each cross-section using the experimental torsion testing. The numbers listed in this row are the largest rupture values.

Rupture typically occurred on one end of the specimen. There was no obvious pattern for either a cross-section or test number. One example of a broken test specimen for each cross-section is depicted in Figure 3.25.

Figure 3.25 6061-T6 rupture specimens.

3.2.5 5052-H32 Results

The 5052-H32 torsion testing results are presented in this section, which report the findings identically to the 6061-T6 series. One difference from the 6061-T6 series study is that there is no circular shape testing completed for this alloy because no vendors could supply the 5052-H32 series in rod form. Therefore, testing was only completed on the square and rectangular bar shapes. The Predicted limit state values are illustrated in Table 3.19, and the ADM predictions are listed in Table 3.20.

Table 3.19 5052-H32 Initial Yield, Full Yield, and Rupture values – Predicted.

	Shape			
	Square	w/t=2	w/t=3	w/t=4
T_y (in-lb.)	305.5	721.6	1,179.6	1,656.5
T_p (in-lb.)	490.0	1,224.9	1,959.9	2,694.9
T_u (in-lb.)	760.4	1,901.0	3,041.6	4,182.2

Table 3.20 6061-T6 Yielding and Rupture values - ADM.

	Shape			
	Square	w/t=2	w/t=3	w/t=4
T_y (in-lb.)	358.5	846.9	1,384.3	1,943.9
T_p (in-lb.)	575.0	1,437.5	2,300.0	3,162.5
T_u (in-lb.)	775.0	1,937.5	3,100.0	4,262.5

3.2.4.1 Initial Yield Results

The plots presented in Figure 3.26 display initial yield values plotted over the experimental torsional data. The solid, black horizontal line corresponds to the initial yield value using the predicted yield strength, 19.60 ksi, whereas the dashed line represents the initial yield value obtained using the yield strength listed in the *Specification for Aluminum Structures*, 23 ksi (ADM).
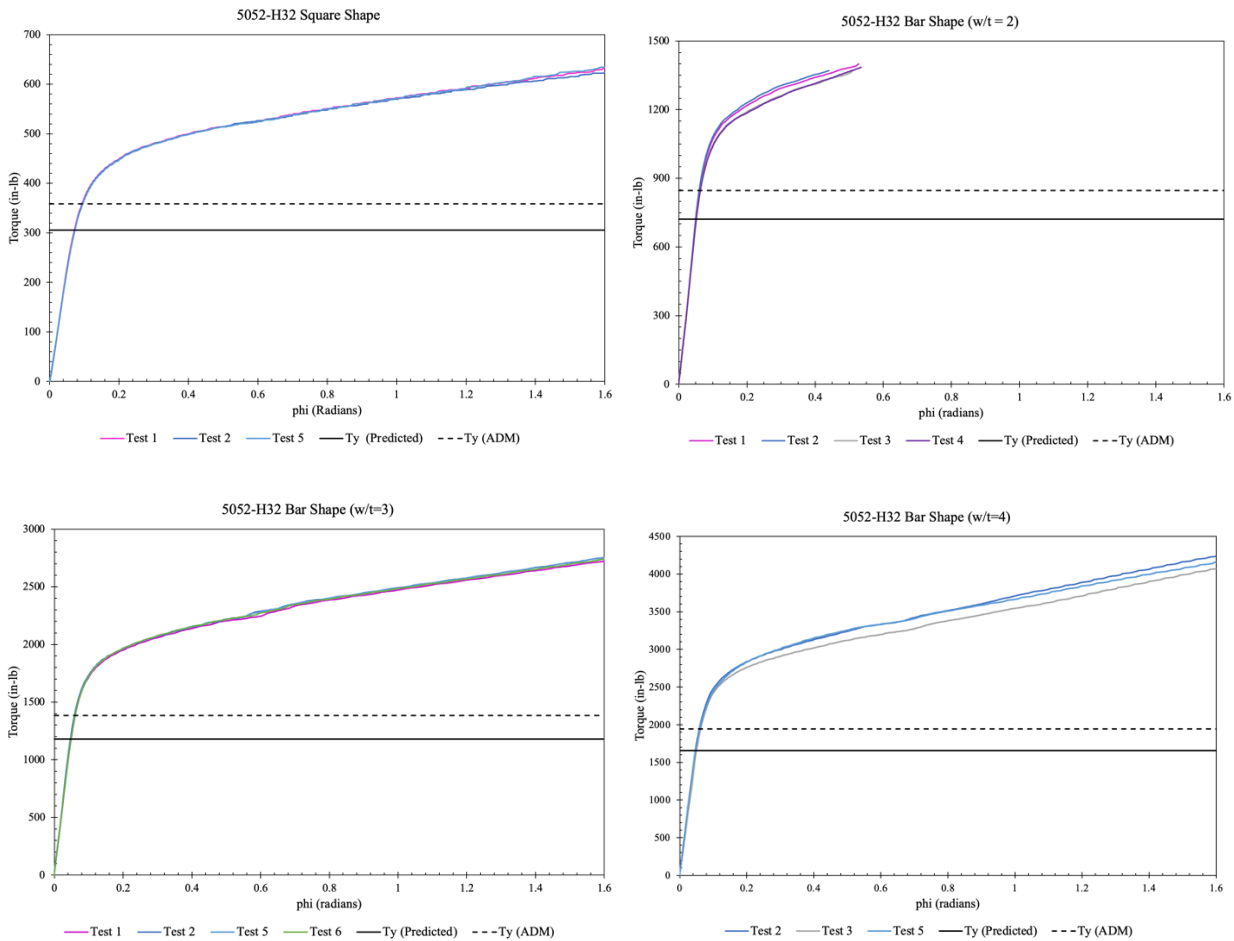
Figure 3.26 5052-H32 Torsion Test results initial yield strength predictions.

3.2.4.2 Full Yield Results

The contents of this section display the torsion data with the full yield estimations plotted over it. This procedure means that the full yield equation presented in Chapter 2 were used for this section. Similar to the previous section, the solid horizontal line correlates to values using a yield strength of 19.60 ksi from tension testing. The dashed horizontal line corresponds to full yield values determined using the 23 ksi yield strength list in the *Specification for Aluminum Structures*. The results are plotted in Figure 3.27.
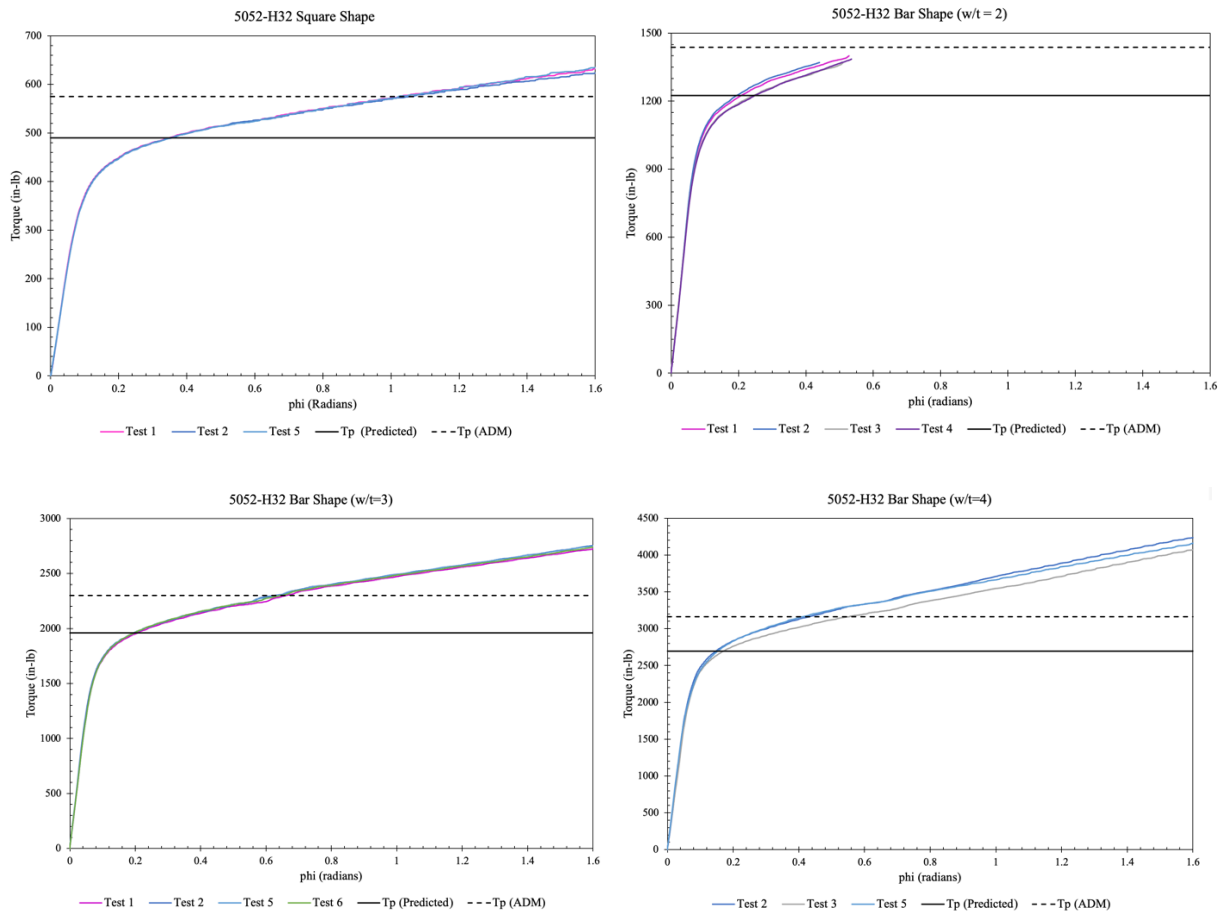
Figure 3.27 5052-H32 Torsion Test results full yield strength predictions.

One obvious observation from these plots is that the bar shape with an aspect ratio of two seems to be missing data. For each test, once the torque applied to the specimen reached roughly 1,350 in-lb., the data became inconsistent. The plot experienced a large jump in the torque values and did not follow the curve path. Furthermore, this inconsistency was different for each test. However, because the data was consistent up until the plot illustrated this jump, so only the data collected after the irregular jump was removed.

3.2.4.3 GJ/L Study Results

The results of the 5052-H32 $\frac{GJ}{L}$ study are presented in this section. This study was conducted following the same procedure as the 6061-T6 series. Similarly, the dashed red line in Figure 3.28 signifies the $\frac{GJ}{L}$ value, and the corresponding value can be found in the box of each plot. Table 3.21 and Table 3.22 present the results of this study in tabular form.
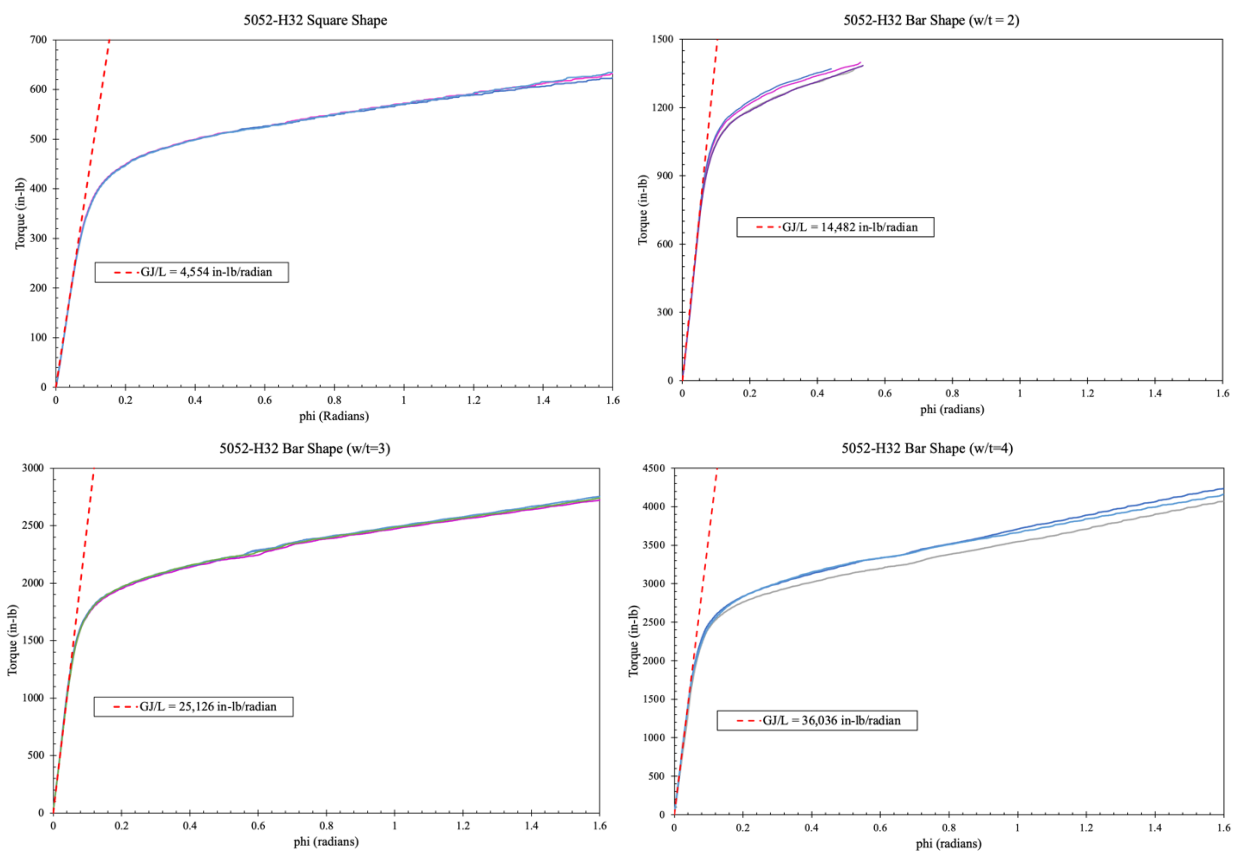
Figure 3.28 5052-H32 $\frac{GJ}{L}$study results.

Table 3.21 5052-H32 $\frac{GJ}{L}$ values.

	Square	w/h=2	w/h=3	w/h=4
Predicted (k-in./radians)	4.78	15.20	26.24	37.31
ADM (k-in./radians)	4.68	15.26	26.34	37.44
Actual (k-in./radians)	4.55	14.48	25.13	36.04

Table 3.22 5052-H32 $\frac{GJ}{L}$ ratios.

	Square	w/h=2	w/h=3	w/h=4
Predicted (k-in./radians)	0.95	0.95	0.96	0.97
ADM (k-in./radians)	0.97	0.95	0.95	0.96

The goal of the numbers listed in Table 3.22 is to be as close to 1 as possible because a ratio of 1 implies that the estimation is the same as the Actual $\frac{GJ}{L}$ value. For both the 6061-T6 and 5052-H32 series, these ratios are close to 1, which indicates that the is data reliable.

3.2.4.3 Rupture Results

The contents of this section outline, present, and compare the 5052-H32 series rupture results. The experimental rupture results from torsion testing are listed in Table 3.23.

Table 3.23 Experimental rupture values for 5052-H32.

	Test 1	Test 2	Test 3	Test 4	Test 5	Test 6
Square	880	878	887	878	893	894
Bar (w/t=2)	2,620	2,630	2,595	2,580	N/A	N/A
Bar (w/t=3)	5,025	5,090	5,075	5,075	5,060	5,080
Bar (w/t=4)	8,480	8,400	8,500	8,680	8,500	N/A

Rupture results were independent of any inclinometer data, so values collected for tests that were removed for yielding results were kept in the results table. The data support this action because the rupture values vary within a reasonable range. The boxes filled with "N/A" correlate to a test where testing concluded before rupture occurred.

Statistical analysis procedures were completed on the findings from these experiments. The mean, standard deviation and median values are present in Table 3.24 and 95% confidence intervals about the mean are illustrated in Table 3.25.

Table 3.24 Statistical Analysis Results for 5052-H32 Experimental Rupture Values.

	Mean	**Std.**	**Median**
Square	885.00	7.38	882.50
Bar (w/t=2)	2,606.25	22.87	2,600.63
Bar (w/t=3)	5,067.50	22.97	5,071.25
Bar (w/t=4)	8,512.00	102.57	8,500.00

An important takeaway from this table is that for the bar's with aspect ratios of two and three have similar standard deviation values. The bar with an aspect ratio of two only displays four rupture

values, meaning that the sample size is smaller. This smaller sample size explains the rational for why these two bars have the same standard deviation.

Table 3.25 Confidence Intervals for Mean Experimental Rupture Results.

	Lower	Mean	Upper
Square (in-lb.)	877.26	885	892.74
Bar (w/t=2) (in-lb.)	2,569.86	2,606.25	2,642.64
Bar (w/t=3) (in-lb.)	5,043.40	5,067.50	5,091.60
Bar (w/t=4) (in-lb.)	8,384.65	8,512.00	8,639.35

The confidence intervals listed in Table 3.25 assume 95% confidence. These ranges suggest that we are 95% confident that the rupture values for various cross-sections using the 5052-H32 material that conducted this study's testing fall within the limits listed in Table 3.25.

Three different rupture values were recorded for each 5052-H32 cross-section: Two equation-based estimations and one experimental observation. Table 3.26 lists these three different values for each cross-section.

Table 3.26 5052-H32 Rupture Results Comparison.

	Square	w/h=2	w/h=3	w/h=4
Predicted (in-lb.)	760.40	1,901.01	3,041.61	4,182.22
ADM (in-lb.)	775	1,937.5	3,100	4,262.5
Actual (in-lb.)	885	2,606.25	5,067.50	8,512.00

Figure 3.29 illustrates four examples of rupture specimens for the 5052-H32 alloy. There is one specimen for each of the four cross-sections used for this study.

Figure 3.29 5052-H32 rupture specimens.

CHAPTER 4: DISCUSSION OF RESULTS

4.1 Summary of Results

The purpose of this section is to examine the results presented in Chapter 3. First, an analysis of each material results, beginning with the 6061-T6 series, will be discussed. Then, a comparison between the two alloy results will be presented. These discussions help introduce the topics needed to draw conclusions that are presented in the next chapter.

4.1.1 6061-T6 Discussion

The results of the 6061-T6 tension tests provide an opportunity to predict the yield and ultimate strengths of the 6061-T6 torsion tests more accurately. Given that the torsion specimens were rupturing at values higher than the ADM estimations, it was expected that tension tests would generate higher strength values than listed in the *Specification for Aluminum Structures*. The predicted yield strength using the tension test results was larger than the specification's yield strength by a factor of 1.33. Similarly, the computed ultimate strength value was 1.20 times greater than the specification value.

Not only do these factors apply to the tension testing results, but also, they apply to the torsion testing results. The ratio of the Predicted estimation over ADM's estimation is indicative of which strength value was used to compute each limit state. For example, the torsional yielding predictions, T_y and T_p, calculated from the experimental results are 1.33 times greater than ADM estimations. Likewise, the experimental rupture predictions are greater than the ADM predictions by a factor of 1.20. Considering the initial yield and full yield values use the yield strength to

predict these limit states, the factors from the torsion tests should match the factor from the tension tests. This same expectation applies to torsional rupture because the ultimate strength is required to compute this value.

The 6061-T6 plots indicate that the predicted strength values collected through tension testing more accurately estimate the torsional limit states. The solid black lines appear to agree with the plot for each cross-section, meaning that the lines intersect the experimental results where expected. The ADM estimations, on the other hand, intersect the experimental data the ADM line appears to still be in the elastic range. Considering the data still behave linearly during this intersection, this assumption is valid. The only plot that raises some concern is the chart for a bar shape with an aspect ratio of three. Both the initial and fully yielded Predicted values intersect the data at higher value relative to the other plots. This skepticism is also illustrated in the rupture results. The bar shape with an aspect ratio of three has a standard deviation nearly two times larger than the standard deviation for the bar shape with an aspect ratio of four. This observation contradicts expectations. The bar shape with an aspect ratio of four is expected to have the largest standard deviation because the rupture values are higher than for a bar shape with an aspect ratio of three. The consequence of such a large standard deviation returns a large confidence interval. Therefore, the confidence interval for the bar shape with an aspect ratio of three is not as creditable as the other rupture confidence intervals.

Interestingly, the circular shape "Predicted" and "ADM" predictions fall between bar prediction values with aspect ratios of two and three. However, the rupture values contradict this analysis. Looking at the actual data, the mean rupture value for the circular shape occurs between the square

bar and bar with an aspect ratio of two. Theoretically, this combination makes more sense given that a circle more closely resembled a square shape than a rectangular shape. This resemblance stems from the fact that the perpendicular planes are equidistant from the centroid for a circle and a square.

Another outcome observed from these results is that the yielding limit states increase as the aspect ratio increases.

4.1.2 5052-H32 Discussion

The 5052-H32 series produce alarming results because the aluminum specification lists a higher yield and ultimate strength than discovered through tension testing. This overestimation raises concerns because the error suggests that the 5052-H32 alloy is stronger than expected. Structural applications employing this inflated strength increases the likelihood of failure because a structure would be designed assuming stronger strength values.

While the strength values and limit state predictions were smaller than anticipated, they were reduced by similar factors. The yield strength decreased by a factor of 0.85, meaning that the yield strength predicted from tension testing, initial yield prediction, and fully yielded predictions were 0.85 times smaller than the ADM estimations. Similarly, the ultimate strength and rupture values calculated using the tension test results were 0.98 time smaller than the ADM predicted values. Again, these reduction factors correctly match based on which yield strength was used.

The predicted initial yield and fully yielded values appear to predict these limit states more accurately. This same methodology, however, does not hold true for the rupture results. In fact, neither estimation, Predicted or ADM, was particularly close to the actual rupture values. For example, for the bar shape with an aspect ratio of four, the observed rupture values were at least double both the Predicted and ADM estimations.

4.2 Comparison

The most glaring difference between the results of these two alloys is the fact that the *Specifications for Aluminum Structures* underestimated the strength of 6061-T6 series and overestimated 5052-H32 alloys' strength. Interestingly, the specifications overestimate the 6061-T6 strength more than the manual underestimates the 5052-H32 strengths. Despite this difference, the ultimate strength values are closer to one than the yield strength values. This observation implies that the ultimate strength predictions are closer to the values listed in the ADM.

Another interesting observation between the two alloys is that the 5052-H32 appeared to reach initial yielding at an earlier phi value than the 6061-T6 series. Reaching initial yielding at an earlier phi indicates that less torque is required to reach initial yielding, explaining the decreased strength and limit state predictions. For the 6061-T6 series, initial yielding occurs between a phi value of 0.11 and 0.14 radians, whereas for the 5052-H32 series, this value ranges between 0.022 and 0.072. These estimates are based off the intersections point with the torsion data and the solid black horizontal line, which correlate to the predictions using the tension testing yield strength predictions. The fully yielded predictions illustrate no consistent intersection point. Therefore, no observation can be made regarding these phi values.

Further analysis of the Predicted initial yield and fully yielded estimations indicates that 5052-H32 Predicted estimations more accurately calculate these values. This assumption stems from visibly looking at both sets of plots for each alloy.

The 5052-H32 series displayed more inconsistent torsion results, however, the tension test results were more precise. This precision is depicted in the confidence intervals for both alloy's yield and ultimate strength predictions. When comparing the ratios of the interval parameter over the mean (i.e. $\frac{\pm 1.44}{46.60}$ for 6061-T6 F_y), the 5052-H32 ratios are at least three times smaller than the 6061-T6 ratios. This observation suggests that the 5052-H32 series collected better tension test data. There is too much variability and inconsistency to notice and similar patterns and claim similar assumptions.

The $\frac{GJ}{L}$ study indicates that the data is reliable because the ratios presented in Table 3.14 and Table 3.22 are reasonably close to 1. An observation of the 6061-T6 series is that the results have a mix of ratios above and below 1. This mix of ratios above and below 1 is important because it suggests that the data is neither over nor under conservative. For the 5052-H32 series, however, all of the ratios are below 1, but are closer to 1, which still support that the results are reliable.

CHAPTER 5: CONCLUSION

5.1 Conclusions

The proposed torsional limit state equations derived in Chapter 2 accurately predict an aluminum alloy's initial and full yield, however, inaccurately estimate an alloy's torsional rupture. Experimental testing confirmed the credibility of these equations because the predictions using the strength values generated through tension testing intersected the Torque plots at the appropriate points, particularly the initial yield predictions. These predictions intersect the torque plot when the graph appears to enter the inelastic range, meaning the experimental torsion data was no longer linear.

The predictions using the specifications yield strength were inaccurate, but do not discredit the limit state equations, rather discredit the strength properties listed in the manual. As a result, the yield equations should be implemented in the next in installment of the Aluminum Design Manual and should be incorporated into finding the controlling limit states. The rupture equation can be included in the specification, but to obtain accurate predictions, further equation investigation is required. Because the equations proved their accuracy, this study confirmed that a factor of safety can be applied to the limit state predictions after using the equations. Like the steel specifications, the *Specification for Aluminum Structures* allows for Allowable Stress Design (ASD) or Load and Resistance Factor Design (LRFD), meaning that different safety factors are applied to limit states depending on the selected design method. Additionally, the safety factor values changes depending on the limit state. Another study could be conducted to find the ASD and LRFD safety factors that should be applied to the torsional limit state values.

Another conclusion discovered through this study is that the strength properties listed in the *Specification for Aluminum Structures* are inconsistent. Tension tests conducted on samples constructed from excess materials confirmed this conclusion. For the 6061-T6 series, the specification underestimates these strength values, whereas the code overestimated the strength properties of the 5052-H32 series. Wrong strength values listed in the manual create several problems. For starters, in terms of the 5052-H32 series, the overestimation for the strength values means that all of the limit state predictions, not just the torsion equations, will produce higher values, suggesting that members are stronger than they actually are. Therefore, the probability of failure increases.

5.2 Limitations

While the results of these tests were consistent based on the alloy being tested, it is important to acknowledge the limitations associated with this research. In general, the sample size for the torsion and tension testing was small. In order for more generalized statements to be made about the alloys contained in the *Specification for Aluminum Structures*, more tests are required and further evidence supporting these claims for different alloys is needed.

The aluminum materials used for this research were collected from two different vendors. There are several of aluminum producers across the country. As a result, these conclusions may not hold true for all aluminum 6061-T6 and 5052-H32 producers. Perhaps other aluminum producer makes their aluminum to match the specifications. In order to test this theory, further research from other companies is required.

5.3 Further Research Opportunities

There exist many further research opportunities regarding this study because a literary review proved that there is no existing research involving the torsional limit states of aluminum. One possible avenue to take this research is to replicate the same study could be replicated on different aluminum alloys to confirm the conclusions regarding the torsion equations. Additionally, the strength values listed in the *Specifications for Aluminum Structures* need to be examined. Further tension testing will enable more solidified conclusions regarding these values to be identified. Repeated tension tests on the alloys selected to conduct this study, alongside tension tests using different alloys, would strengthen or invalidate the conclusions found in this study.

BIBLIOGRAPHY

Aluminum Association. (2020). *Aluminum design manual*. The Association.

American Society and Testing and Materials. (2021). *Standard Specification for Aluminum-Alloy 6061-T6 Standard Structural Profiles* (02.02 B07.03 - 2020). ASTM International.

American Society and Testing and Materials. (2022). *Standard Test Methods for Tension of Metallic Materials* (03.01 E28.04 - 2022). ASTM International.

American Society and Testing and Materials. (2021). *Standard Test Method for Shear Modulus at Room Temperature* (03.01 E143.20 - 2021). ASTM International.

American Society and Testing and Materials. (2021). *Standard Test Method for Torsion Testing of Wire* (01.03 A938.18 - 2021). ASTM International.

Budynas, R. G., & Sadegh, A. M. (2020). *Roark's formulas for stress and strain*. McGraw-Hill Education.

Kissell, J. R., & Ferry, R. L. (2002). *Aluminum structures: a guide to their specifications and design*. John Wiley & Sons.

Kissell, J. R., & Ziemian, R. D. (2020, February 1). The 2020 Aluminum Design Manual. *Strucutres*, 9-11. https://www.structuremag.org/wp-content/uploads/2020/01/272002-C-StructuralSpecifications-Kissell.pdf

Simcoe, C. R. (2018). *The History of Metals in America*. ASM International.

Ugural, A. C., & Fenster, S. K. (2011). *Advanced mechanics of materials and applied elasticity*. Pearson Education.

APPENDIX

Polar Moment of Inertia Equations:
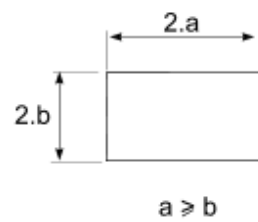
Solid Circular Section

$$J' = \frac{1}{2}\pi.r^4$$

Solid Square Section

$$J' = 2{,}25.a^4$$

Solid Rectangular Section

$$J' = a.b^3\left[\frac{16}{3} - 3{,}36\frac{b}{a}\left(1 - \frac{b^4}{12.a^4}\right)\right]$$

$a \geqslant b$

Testing Procedure for Tension Machine:

The tension tests performed on the specimens were in accordance with the ASTM standards for Tension Testing of Metallic Materials.

Preparing Specimen and Machine for Testing:

1. Measure the dimensions of the tension specimen using the dial caliper.

2. Use a spacer to hammer a 2 in. space into the tension specimen.

3. Login computer and open Bluehill Universal

4. Select desired test (i.e. "MSM Tension Test").

5. The machine should now be up and running.

6. Using the machine's control panel on the right, push the down arrow until the space between the grip matches the gauge distance on the specimen.

7. Place the specimen into the tension machine.

8. To ensure that the specimen is straight in the machine, place a parallel straightening bar in the grips. Have one side of the bar touch the specimen and the other side be even with the ends of the grips so that the bar and grips form a flat surface.

9. Tighten the grips following the direction of the arrow on the machine

10. To apply the Instron accelerometer onto the machine, squeeze the two round circles.

11. Place the device against the testing specimen so that 1 in. gap on the accelerometer is vertical.

12. Use the small black rubber bands to secure the accelerometer - the rubber bands should be applied horizontally (i.e. there should be one band on the top and one on the bottom)

13. The tension sample is now ready to be tested

Running the Test:

1. Go to the computer and click on the tab "Method"

2. Check the dimensions match the ones listed. If not, click on the pencil to edit the dimensions.

3. Using the dial on the control panel, scroll up or down to get the applied load (number in the top middle box) as close to zero as possible.

4. Click the"Before Test" arrow in the bottom right corner.

5. Hit the "Zero all Dimensions" button in the bottom left corner.

6. Wait a few seconds, then select the "Begin Test" button.

7. The machine will then begin testing the specimen.

8. Once the specimen reaches 8% elongation, the test will halt.

9. While the test is not running, squeeze the circles on the accelerometers and remove the bands.

10. Hit the "Continue Testing" button once the accelerometer is removed.

11. The test will then run until failure.

12. Once failure occurs, click on the checkered flag to finish testing. If you need to run another test hit the "yes" button on the pop up window; otherwise, hit no.

13. The data should be saved to your public folder. It is recommended to check your public folder for this data to ensure that the data was collected before logging out of the computer.

14. Remove the specimen from the machine by loosening the grips in the opposite direction that is specified on the machine.

- If more testing is required, do not move the grips up ad down to alleviate extra work for each run

15. Once the specimen is removed from the machine, measure the new gauge length using the dial caliper specifically for tension specimens - note the new gauge length. This value will be used to find the percent elongation.

16. Mark the top and bottom of the specimen and tape the two pieces together. Put the test number and date on the specimen.

17. Store the specimen somewhere for safe keeping.

Testing Procedure for Torsion Machine

Procedure:

Preparing the Specimen:

1. Draw a straight line down the middle of the specimen.

   - For round specimens, I suggest laying the specimen on a flat surface and sliding a sharpie down along the length of the specimen.

   -For flat specimens, mark the middle of the width and using a straight edge, connect the two points.

2. Cut a strip of double-sided tape and put on accelerometer with angled grip attached

3. Place one accelerometer onto specimen using double-sided tape and small angled grips

   Important: Face the accelerometer so that the x axis line faces the left side of the torsion machine and the y-axis line is facing outward from the machine.

4. Put spacer (6 in. tension specimen) against the edge of the accelerometer on the specimen.

5. Place the edge of other accelerometer at the end of the spacer so that both accelerometers are touching the tension member

6. Quickly check to make sure that both accelerometers have the exact same orientation.

7. Specimen is now ready to be tested.

Preparing Machine:

1. Turn on machine - lever on the bottom right corner on the back of the machine

2. Set to desired scale (i.e 6000 in-lb)

3. Set angle on the right twister to zero

4. Place prepared specimen in the right grip.

5. Place 11 in. pvc pipe against the right grip and use orange roller to bring the left grip closer until the left grip touches the pvc pipe.

6. Tighten the left side enough to hold the specimen in place, but not to capacity. One to two twists should be enough.

7. Tighten right side of the machine to its capacity (the hollow rod is useful for this process)

8. Zero the torsional machine using black knob for 6000 in-lb scale.

9. Tighten the loose left side of the machine to its capacity.

10. Torque will likely be applied to the specimen as a result of step 9, so zero machine using clockwise/counterclockwise knobs on the machine. Make sure rpm is set to approximately zero as the machine will reach zero quite fast.

11. When ready to begin test, use opposite of what was used to zero machine (i.e. if counterclockwise was used, run test on the clockwise setting)

12. Now set the machine to 5 rpm

13. You are now ready to prepare accelerometers.

Preparing Accelerometers and Running Test:

1. Turn on all of the accelerometers. Two on specimens and one on a gear on the back othe the machine. A blue light should appear when it's on.

2. Open MiniMu software three times - once for each accelerometer being used.

3. Where the software says "Port" click the down arrow and set one window to "COM3", "COM4," and "COM5" respectively.

- Note which side is "COM4" and which is "COM5." This will simplify the saving process and future calculations

4. Once the accelerometers have been found, select the "config" header.

- Specimen accelerometer: set the algorithm option to "6-axis" and hit acceleration

- Gear accelerometer: set algorithm to "6-axis," install directions to "vertical," and hit acceleration.

5. Click "Save Config" and exited out pop-up window

6. Once all of the accelerometers have been calibrated and zeroed, you are ready to begin recording data.

7. Click "Record" and then begin.

8. Once all three accelerometers are collecting data, push the appropriate button to begin the test.

Ending Test:

1. Once the torsion machine begins to stall (the dial gauge showing the torque appears to be stagnant), you may stop recording data by clicking "stop" under the recording tab.

2. Save the files for future reference.

*Name the files so that it is easy to reference what file is the gear's data, the one on the left side of the specimen, and the one on the right side of the specimen.

3.   Remove the accelerometers from the specimen and turn them off.

4.   Keep the machine running so that the test continues until rupture.

5.   Watch the machine and note the highest torque value reached before rupture.

6.   Once rupture occurs, stop the machine by pushing the red button. Record the final angle

of rotation using the angle measurer on the machine. Note that you may have to perform some

calculations because the machine only represents 360 degrees.

7.   Remove broken specimen from both sides of the machine.

8.   Set the angle on the torsion machine back to zero.

9.   Repeat all procedures to perform next if needed.

Designation: B308/B308M – 20

Standard Specification for
Aluminum-Alloy 6061-T6 Standard Structural Profiles[1]

This standard is issued under the fixed designation B308/B308M; the number immediately following the designation indicates the year of original adoption or, in the case of revision, the year of last revision. A number in parentheses indicates the year of last reapproval. A superscript epsilon (ε) indicates an editorial change since the last revision or reapproval.

This standard has been approved for use by agencies of the U.S. Department of Defense.

1. Scope*

1.1 This specification[2] covers extruded 6061-T6 aluminum-alloy standard structural profiles.

1.2 The profiles are limited to I-beams, H-beams, channels, angles, tees, and zees.

NOTE 1—For other extruded profiles in other alloys and tempers refer to Specification B221.

1.3 Alloy and temper designations are in accordance with ANSI H35.1/H35.1(M). The equivalent Unified Numbering System alloy designation is that in Table 1 preceded by A9, or A96061 for alloy 6061 in accordance with Practice E527.

1.4 For acceptance criteria for inclusion of new aluminum and aluminum alloys in this specification, see Annex A2.

1.5 The values stated in either SI units or inch-pound units are to be regarded separately as standard. The values stated in each system may not be exact equivalents; therefore, each system shall be used independently of the other. Combining values from the two systems may result in non-conformance with the standard.

1.6 *This standard does not purport to address all of the safety concerns, if any, associated with its use. It is the responsibility of the user of this standard to establish appropriate safety, health, and environmental practices and determine the applicability of regulatory limitations prior to use.*

1.7 *This international standard was developed in accordance with internationally recognized principles on standardization established in the Decision on Principles for the Development of International Standards, Guides and Recommendations issued by the World Trade Organization Technical Barriers to Trade (TBT) Committee.*

2. Referenced Documents

2.1 The following documents of the issue in effect on the date of material purchase form a part of this specification to the extent referenced herein:

2.2 *ASTM Standards:*[3]

B221 Specification for Aluminum and Aluminum-Alloy Extruded Bars, Rods, Wire, Profiles, and Tubes

B557 Test Methods for Tension Testing Wrought and Cast Aluminum- and Magnesium-Alloy Products

B557M Test Methods for Tension Testing Wrought and Cast Aluminum- and Magnesium-Alloy Products (Metric)

B647 Test Method for Indentation Hardness of Aluminum Alloys by Means of a Webster Hardness Gage

B648 Test Method for Indentation Hardness of Aluminum Alloys by Means of a Barcol Impressor

B660 Practices for Packaging/Packing of Aluminum and Magnesium Products

B666/B666M Practice for Identification Marking of Aluminum and Magnesium Products

B807/B807M Practice for Extrusion Press Solution Heat Treatment for Aluminum Alloys

B881 Terminology Relating to Aluminum- and Magnesium-Alloy Products

B918 Practice for Heat Treatment of Wrought Aluminum Alloys

B985 Practice for Sampling Aluminum Ingots, Billets, Castings and Finished or Semi-Finished Wrought Aluminum Products for Compositional Analysis

D3951 Practice for Commercial Packaging

E18 Test Methods for Rockwell Hardness of Metallic Materials

E29 Practice for Using Significant Digits in Test Data to Determine Conformance with Specifications

E527 Practice for Numbering Metals and Alloys in the Unified Numbering System (UNS)

---

[1] This specification is under the jurisdiction of ASTM Committee B07 on Light Metals and Alloys and is the direct responsibility of Subcommittee B07.03 on Aluminum Alloy Wrought Products.

Current edition approved Jan. 1, 2020. Published January 2020. Originally approved in 1956. Last previous edition approved in 2010 as B308/B308M – 10 which was withdrawn January 2019 and reinstated January 2020, DOI: 10.1520/B0308_B0308M-20.

[2] For ASME Boiler and Pressure Vessel Code applications see related Specification SB-308 in Section II of that Code.

[3] For referenced ASTM standards, visit the ASTM website, www.astm.org, or contact ASTM Customer Service at service@astm.org. For *Annual Book of ASTM Standards* volume information, refer to the standard's Document Summary page on the ASTM website.

---

*A Summary of Changes section appears at the end of this standard

E607 Test Method for Atomic Emission Spectrometric Analysis Aluminum Alloys by the Point to Plane Technique Nitrogen Atmosphere (Withdrawn 2011)[4]

E716 Practices for Sampling and Sample Preparation of Aluminum and Aluminum Alloys for Determination of Chemical Composition by Spark Atomic Emission Spectrometry

E1251 Test Method for Analysis of Aluminum and Aluminum Alloys by Spark Atomic Emission Spectrometry

E3061 Test Method for Analysis of Aluminum and Aluminum Alloys by Inductively Coupled Plasma Atomic Emission Spectrometry (Performance Based Method)

2.3 *ANSI Standards:*

H35.1/H35.1(M) Alloy and Temper Designation Systems for Aluminum[5]

H35.2 Dimensional Tolerances for Aluminum Mill Products[5]

H35.2(M) Dimensional Tolerances for Aluminum Mill Products (Metric)[5]

2.4 *Federal Standard:*

Fed. Std. No. 123 Marking for Shipment (Civil Agencies)[6]

2.5 *AMS Specifications:*

AMS 2772 Heat Treatment of Aluminum Alloy/Raw Materials[7]

2.6 *Military Specifications:*

MIL-STD-129 Marking for Shipment and Storage[6]

2.7 *CEN EN Standards:*

EN 14242 Aluminum and aluminum alloys, Chemical analysis inductively coupled plasma optical emission spectral analysis.[8]

3. Terminology

3.1 *Definitions*—Refer to Terminology B881 for definitions of product terms used in this specification.

3.2 *Definitions of Terms Specific to This Standard:*

3.2.1 *inspection lot*—an identifiable quantity of material of the same mill form, alloy, temper, and nominal dimensions traceable to a heat-treat lot of lots, subjected to inspection at one time (see 14.1).

3.2.2 *heat-treat lot*—an identifiable quantity of material heat-treated in the same furnace at the same time (see 10.2.1 and 10.2.2).

4. Ordering Information

4.1 Orders for material to this specification shall include the following information:

4.1.1 This specification designation (which includes the number, the year, and the revision letter, if applicable),

NOTE 2—For inch-pound orders specify B308; for metric orders specify B308M. Do not mix units.

4.1.2 Quantity in pieces or pounds [kilograms],

4.1.3 Alloy (Section 8),

4.1.4 Temper (10.1 and Table 2),

4.1.5 Type of section (1.2), dimensions (including a drawing if necessary), and length,

4.2 Additionally, orders for material to this specification shall include the following information when required by the purchaser:

4.2.1 Whether solution heat treatment at the extrusion press is unacceptable (9.2),

4.2.2 Whether heat treatment in accordance with Practice B918 is required (9.3),

4.2.3 Whether inspection or witness of inspection and tests by the purchaser's representative is required prior to material shipment (Section 13),

4.2.4 Whether certification of the material by the supplier is required (Section 15),

4.2.5 Whether marking for identification is required (16.1), and

4.2.6 Whether Practices B660 applies and, if so, the applicable levels of preservation, packaging, and packing required (17.3).Table 2

5. Materials and Manufacture

5.1 The products covered by this specification shall be produced by hot extruding only.

TABLE 1 Chemical Composition Limits[A,B,C,F]

Alloy 6061	Composition, %
Silicon	0.40–0.8
Iron	0.7
Copper	0.15–0.40
Manganese	0.15
Magnesium	0.8–1.2
Chromium	0.04–0.35
Zinc	0.25
Titanium	0.15
Other elements[D] each	0.05
Total[E]	0.15
Aluminum	rem

[A] Where single units are shown, these indicate the maximum amounts permitted.

[B] Analysis shall be made for the elements for which limits are shown in this table.

[C] For purposes of determining conformance to these limits, an observed value or a calculated value obtained from analysis shall be rounded to the nearest unit in the last right-hand place of figures used in expressing the specified limit, in accordance with the rounding-off method of Practice E29.

[D] *Others* includes all unlisted metallic elements. The producer may analyze samples for trace elements not specified in the specification. However, such analysis is not required and may not cover all metallic *Others* elements. Should any analysis by the producer or the purchaser establish that an *Others* element exceeds the limit of *Each* or that the aggregate of several *Others* elements exceeds the limit of *Total*, the material shall be considered nonconforming.

[E] *Other Elements*—Total shall be the sum of unspecified metallic elements 0.010 % or more, rounded to the second decimal before determining the sum.

[F] In case there is a discrepancy in the values listed in Table 1 with those listed in the "International Alloy Designations and Chemical Composition Limits for Wrought Aluminum and Wrought Aluminum Alloys" (known as the "Teal Sheets"), the composition limits registered with the Aluminum Association and published in the "Teal Sheets" shall be considered the controlling composition. The "Teal Sheets" are available at http://www.aluminum.org/tealsheets.

[4] The last approved version of this historical standard is referenced on www.astm.org.

[5] Available from Aluminum Association, Inc., 1400 Crystal Dr., Suite 430, Arlington, VA 22202, http://www.aluminum.org.

[6] Available from Standardization Documents Order Desk, DODSSP, Bldg. 4, Section D, 700 Robbins Ave., Philadelphia, PA 19111-5098, http://dodssp.daps.dla.mil.

[7] Available from SAE International (SAE), 400 Commonwealth Dr., Warrendale, PA 15096-0001, http://www.sae.org.

[8] Available from European Committee for Standardization (CEN), 36 rue de Stassart, B-1050, Brussels, Belgium, http://www.cenorm.be.

TABLE 2 Tensile Property Limits[A,B]

	6061-T6
Tensile strength, min, ksi [MPa]	38.0 [260]
Yield strength, min, ksi [MPa]	35.0 [240]
Elongation,[C] min, %	
in 2 in. [50 mm]	10 [10][D]
in 4D [5D or 5.65 $\sqrt{A}$]	10 [9]

[A] For purposes of determining conformance with this specification, each value for tensile strength and yield strength shall be rounded to the nearest 0.1 ksi [1 MPa], and each value for elongation shall be rounded to the nearest 0.5 %, both in accordance with the rounding method of Practice E29.

[B] The basis for mechanical property limits is given in Annex A1.

[C] Elongations in 2 in. [50 mm] apply for profiles tested in full section and for sheet-type specimens machined from material up through 0.500 in. [12.5 mm] in thickness having parallel surfaces. Elongations in 4D [5D or 5.65 $\sqrt{A}$], where D and A are diameter and cross-sectional area of the specimen, respectively, apply to round test specimens machined from thicknesses over 0.250 in. [6.30 mm].

[D] For thicknesses less than 0.250 in. [up through 6.30 mm] the minimum elongation is 8 %.

6. Quality Assurance

6.1 *Responsibility for Inspection and Tests*—Unless otherwise specified in the contract or purchase order, the producer is responsible for the performance of all inspection and test requirements specified herein. The producer may use his own or any other suitable facilities for the performance of the inspection and test requirements specified herein, unless disapproved by the purchaser in the order or at the time of contract signing. The purchaser shall have the right to perform any of the inspections and tests set forth in this specification where such inspections are deemed necessary to ensure that material conforms to prescribed requirements.

7. General Quality

7.1 Unless otherwise specified, the structural profiles shall be supplied in the mill finish and shall be uniform as defined by the requirements of this specification and shall be commercially sound. Any requirement not so covered is subject to negotiation between the producer and purchaser.

7.2 Each profile shall be examined to determine conformance to this specification with respect to general quality and identification marking. On approval of the purchaser, however, the producer or the supplier may use a system of statistical quality control for such examination.

8. Chemical Composition

8.1 *Limits*—The material shall conform to the chemical composition limits specified in Table 1. Conformance shall be determined by the producer by taking samples in accordance with E716 when the ingots are poured, and analyzing those samples in accordance with E607, E1251, E3061, or EN 14242. At least one sample shall be taken for each group of ingots poured simultaneously from the same source of molten metal. If the producer has determined the chemical composition during pouring of the ingots, they shall not be required to sample and analyze the finished product.

8.2 If it becomes necessary to analyze an extrusion for conformance to chemical composition limits, the methods of sampling and methods of analysis shall be as provided in the following:

8.2.1 *Methods of Sampling*—Samples for chemical analysis shall be taken in accordance with Practice B985.

8.2.2 *Methods of Analysis*—Analysis shall be performed in accordance with Test Methods E607, E1251, E3061, or EN 14242.

8.3 Other methods of analysis or in the case of dispute may be by agreement between the producer and the purchaser.

NOTE 3—It is standard practice in the United States aluminum industry to determine conformance to the chemical composition limits prior to further processing of ingots into wrought products. Due to the continuous nature of the process, it is not practical to keep a specific ingot analysis identified with a specific quantity of finished material.

9. Heat Treatment

9.1 Except as noted in 9.2, or otherwise specified in 9.3, producer or supplier heat treatment shall be in accordance with AMS 2772.

9.2 Unless otherwise specified, material may be solution heat-treated and quenched at the extrusion press in accordance with Practice B807/B807M.

9.3 When specified, heat treatment shall be in accordance with Practice B918.

10. Tensile Properties

10.1 *Limits*—The structural profiles shall conform to the tensile requirements specified in Table 2.

10.1.1 The elongation requirements shall not be applicable to the following:

10.1.1.1 Material of such dimensions that a standard test specimen cannot be taken in accordance with Test Methods B557 or B557M and of such profile that it cannot be satisfactorily tested in full section.

10.1.1.2 Material less than 0.062 in. [up through 1.60 mm] in thickness.

10.2 *Number of Specimens:*

10.2.1 For material having a nominal weight of less than 1 lb/linear ft [up through 1.7 kg/linear m], one tension test specimen shall be taken for each 1000 lb [500 kg] or fraction thereof in the heat-treat lot.

10.2.2 For material having a nominal weight of 1 lb or more/linear ft [over 1.7 kg/linear m], one tension test specimen shall be taken for each 1000 ft [300 m] or fraction thereof in the heat-treat lot.

10.2.3 Other procedures for selecting samples may be employed if agreed upon by the producer and the purchaser.

10.3 *Test Specimens:*

10.3.1 *Tension Specimens*—Tension test specimens shall conform to Test Methods B557 or B557M.

10.4 *Test Method:*

10.4.1 *Tension Tests*—The tension test shall be made in accordance with Test Methods B557 or B557M.

11. Quality Assurance Screening of Extrusion Press Heat-Treated Shapes

11.1 For 6061-T6 shapes that are manufactured by quenching at the extrusion press, the requirements of this section shall

apply in addition to all other applicable requirements of this specification. Hardness tests shall be performed either on each extruded charge or on a sample selected in accordance with a sampling plan as specified on purchase orders. The minimum hardness control value shall be in accordance with Table 3 for the type of hardness tester used. The specific type of hardness tester used shall be the producer's choice. The test shall be conducted in accordance with the applicable hardness test standard, namely Test Method B647 for Webster hardness, Test Method B648 for Barcol hardness, or Test Methods E18 for Rockwell E hardness.

11.2 Individual extruded charges that fail to conform to the requirements of Table 3 may be accepted provided the two pieces in the lot having the two lowest hardness readings are tension-tested and found to conform to the requirements of Table 2.

12. Dimensional Tolerances

12.1 Unless otherwise specified, structural profiles ordered to this specification shall meet the requirements of ANSI H35.2/H35.2(M).

13. Source Inspection

13.1 If the purchaser desires that his representative inspect or witness the inspection and testing of the material prior to shipment, such agreement shall be made by the purchaser and producer as part of the purchase contract.

13.2 When such inspection or witness of inspection and testing is agreed upon, the producer shall afford the purchaser's representative all reasonable facilities to satisfy him that the material meets the requirements of this specification. Inspection and tests shall be conducted so there is no unnecessary interference with the producer's operations.

TABLE 3 Hardness Screening Values[A,B,C]

Thickness		Hardness Number, min		
in.	mm	Webster	Barcol	Rockwell E
0.050 through 0.075	over 1.20 through 2.00	15	76	89
0.076 through 0.499	over 2.00 through 12.50	15	76	90
0.500 and over	over 12.50	...	76	...

[A] See Section 11.
[B] Alternate minimum hardness values and hardness testing devices may be used provided that agreement is reached between the purchaser and the supplier or producer.
[C] The hardness values shown do not guarantee material will pass the applicable mechanical property requirements but are for informational purposes only. It is the responsibility of the user of this specification to establish the relationship between the hardness values and tensile properties.

14. Rejection and Retest

14.1 If any material fails to conform to all of the applicable requirements of this specification, it shall be cause for rejection of the inspection lot.

14.2 When there is evidence that a failed specimen was not representative of the inspection lot and when no other sampling plan is provided or approved by the purchaser through the contract or purchase order, retesting may be performed in accordance with Section 9 of Test Methods B557 and B557M.

14.3 Material in which defects are discovered subsequent to inspection may be rejected.

14.4 If material is rejected by the purchaser, the producer or supplier is responsible only for replacement of the material to the purchaser. As much as possible of the rejected material shall be returned to the producer or supplier.

15. Certification

15.1 The producer or supplier shall, on request, furnish to the purchaser a certificate stating that each lot has been sampled, tested, and inspected in accordance with this specification, and has met the requirements.

16. Identification Marking of Product

16.1 When marking for identification is required (see 4.2.5), all material shall be marked in accordance with Practice B666/B666M.

17. Packaging and Package Marking

17.1 The material shall be packaged to provide adequate protection during normal handling and transportation, and each package shall contain only one size, alloy, and temper of material unless otherwise agreed upon. The type of packaging and gross weight of containers shall, unless otherwise agreed upon, be at the producer's discretion, provided that they are such as to ensure acceptance by common or other carriers for safe transportation at the lowest rate to the delivery point.

17.2 Each shipping container shall be marked with the purchase order number, material size, specification number, alloy and temper, gross and net weights, and the producer's name or trademark.

17.3 When specified in the contract or purchase order, material shall be preserved, packaged, and packed in accordance with the requirements of Practices B660. The applicable levels shall be as specified in the contract or order. Marking for shipment of such material shall be in accordance with Fed. Std. No. 123 and Practice D3951 for civil agencies and MIL-STD-129 for military agencies.

18. Keywords

18.1 aluminum alloy; standard structural profiles

Advanced Mechanics of Materials and Applied Elasticity

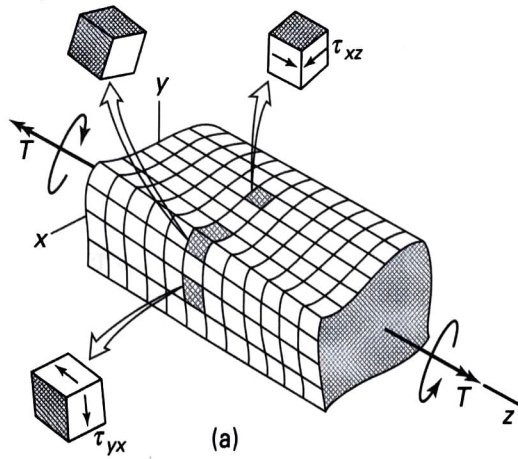## Fifth Edition

ANSEL C. UGURAL

SAUL K. FENSTER

FIGURE 6.13. *Example 6.5. Deformation and stress in a rectangular bar segment under torsion. Note that the original plane cross sections have warped out of their own plane.*

point. The values of the maximum shearing stress τ_{max} in a rectangular cross section and the angle of twist per unit length θ are given in the next section (see Table 6.2).

Interestingly, a *corner element* of the cross section of a rectangular shaft under torsion does not distort at all, and hence the shear stresses are zero at the corners, as illustrated in Fig. 6.13. This is possible because outside surfaces are free of all stresses. The same considerations can be applied to the other points on the boundary. The shear stresses acting on three *outermost* cubic elements isolated from the bar are illustrated in the figure. Here stress-free surfaces are indicated as shaded. Observe that all shear stresses τ_{xy} and τ_{xz} in the plane of a cut near the boundaries act on them.

6.6 PRANDTL'S MEMBRANE ANALOGY

It is demonstrated next that the differential equation for the stress function, Eq. (6.9), is of the same form as the equation describing the deflection of a membrane or soap film subject to pressure. Hence, an analogy exists between the torsion and membrane problems, serving as the basis of a number of experimental techniques. Consider an edge-supported homogeneous membrane, given its boundary contour by a hole cut in a plate (Fig. 6.14a). The *shape* of the hole is the same as that of the twisted bar to be studied; the *sizes* need not be identical.

Equation of Equilibrium

The equation describing the z deflection of the membrane is derived from considerations of equilibrium applied to the isolated element *abcd*. Let the tensile forces per unit membrane length be denoted by S. From a small z deflection, the
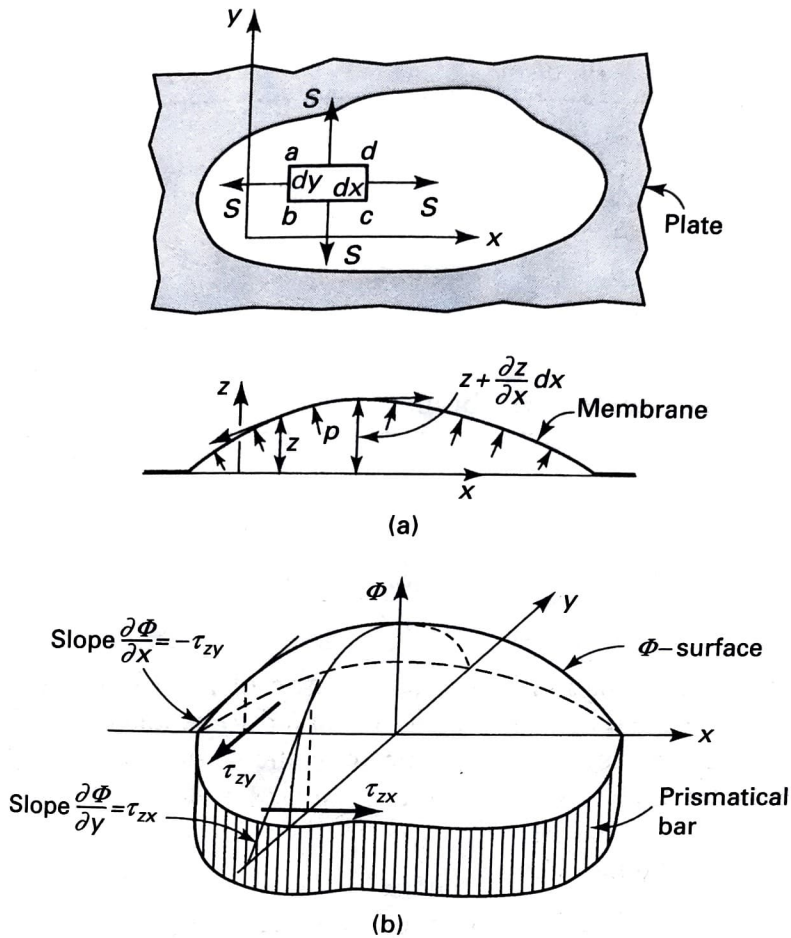
FIGURE 6.14. *Membrane analogy for torsion members of solid cross section.*

inclination of S acting on side ab may be expressed as $\beta \approx \partial z/\partial x$. Since z varies from point to point, the angle at which S is inclined on side dc is

$$\beta + \frac{\partial \beta}{\partial x} dx \approx \frac{\partial z}{\partial x} + \frac{\partial^2 z}{\partial x^2} dx$$

Similarly, on sides ad and bc, the angles of inclination for the tensile forces are $\partial z/\partial y$ and $\partial z/\partial y + (\partial^2 z/\partial y^2) dy$, respectively. In the development that follows, S is regarded as a constant, and the weight of the membrane is ignored. For a uniform lateral pressure p, the equation of vertical equilibrium is then

$$-(S\,dy) \frac{\partial z}{\partial x} + S\,dy \left(\frac{\partial z}{\partial x} + \frac{\partial^2 z}{\partial x^2} dx \right) - (S\,dx) \frac{\partial z}{\partial y}$$

$$+ (S\,dx)\left(\frac{\partial z}{\partial y} + \frac{\partial^2 z}{\partial y^2} dy \right) + p\,dx\,dy = 0$$

TABLE 6.1   *Analogy between Membrane and Torsion Problems*

Membrane Problem	Torsion Problem
z	Φ
$\dfrac{1}{S}$	G
p	2θ
$-\dfrac{\partial z}{\partial x},\ \dfrac{\partial z}{\partial y}$	$\tau_{zy},\ \tau_{zx}$
$2\cdot$ (volume beneath membrane)	T

leading to

$$\frac{\partial^2 z}{\partial x^2} + \frac{\partial^2 z}{\partial y^2} = -\frac{p}{S} \tag{6.15}$$

This is again Poisson's equation. Upon comparison of Eq. (6.15) with Eqs. (6.9) and (6.8), the quantities shown in Table 6.1 are observed to be analogous. The membrane, subject to the conditions outlined, thus represents the Φ surface (Fig. 6.14b). In view of the derivation, the restriction with regard to smallness of slope must be borne in mind.
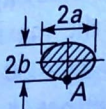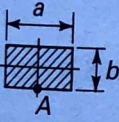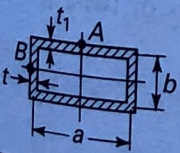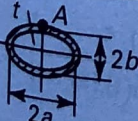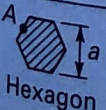
Shearing Stress and Angle of Twist

We outline next one method by which the foregoing theory can be reduced to a useful experiment. In two thin, stiff plates, bolted together, are cut two adjacent holes; one conforms to the outline of the irregular cross section and the other is circular. The plates are then separated and a thin sheet of rubber stretched across the holes (with approximately uniform and equal tension). The assembly is then bolted together. Subjecting one side of the membrane to a uniform pressure p causes a different distribution of deformation for each cross section, with the circular hole providing calibration data. The measured geometric quantities associated with the circular hole, together with the known solution, provide the needed proportionalities between pressure and angle of twist, slope and stress, volume and torque. These are then applied to the irregular cross section, for which the measured slopes and volume yield τ and T. The need for precise information concerning the membrane stress is thus obviated.

The membrane analogy provides more than a useful *experimental* technique. As is demonstrated in the next section, it also serves as the basis for obtaining approximate *analytical* solutions for bars of narrow cross section as well as for members of open thin-walled section.

For reference purposes, Table 6.2 presents the shearing stress and angle of twist for a number of commonly encountered shapes [Ref. 6.4]. Note that the values of coefficients α and β depend on the ratio of the length of the long side or depth a to the width b of the short side of a rectangular section. For thin sections, where a is much greater than b, their values approach 1/3. We observe that, in all cases, the maximum shearing stresses occur at a point on the edge of the cross section that is closest to the

TABLE 6.2 Shear Stress and Angle of Twist of Various Members in Torsion

Cross section	Maximum shearing stress	Angle of twist per unit length
2a, 2b, A For circular bar: $a = b$	$\tau_A = \dfrac{2T}{\pi ab^2}$	$\theta = \dfrac{(a^2 + b^2)T}{\pi a^3 b^3 G}$
Equilateral triangle	$\tau_A = \dfrac{20T}{a^3}$	$\theta = \dfrac{46.2T}{a^4 G}$
a, b, A	$\tau_A = \dfrac{T}{\alpha ab^2}$	$\theta = \dfrac{T}{\beta ab^3 G}$

a/b	β	α
1.0	0.141	0.208
1.5	0.196	0.231
2.0	0.229	0.246
2.5	0.249	0.256
3.0	0.263	0.267
4.0	0.281	0.282
5.0	0.291	0.292
10.0	0.312	0.312
∞	0.333	0.333

Cross section	Maximum shearing stress	Angle of twist per unit length
t_1, A, B, t, b, a	$\tau_A = \dfrac{T}{2abt_1}$ $\tau_B = \dfrac{T}{2abt}$	$\theta = \dfrac{(at + bt_1)T}{2tt_1 a^2 b^2 G}$
t, A, 2b, 2a For circular tube: $a = b$	$\tau_A = \dfrac{T}{2\pi abt}$	$\theta = \dfrac{\sqrt{2(a^2 + b^2)}T}{4\pi a^2 b^2 t G}$
A, a Hexagon	$\tau_A = \dfrac{5.7T}{a^3}$	$\theta = \dfrac{8.8T}{a^4 G}$

center axis of the shaft. A *circular shaft* is the most efficient; it is subjected to both smaller maximum shear stress and a smaller angle of twist than the corresponding noncircular shaft of the same cross-sectional area and carrying the same torque.

6.6   Prandtl's Membrane Analogy

FIGURE 12.20. *Example 12.11. (a) A frame with concentrated loads; (b and c) mechanism of collapse with plastic hinges at A, B, C, and D.*
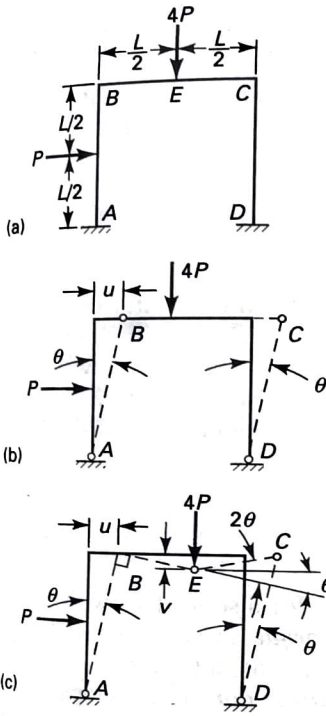
12.9 ELASTIC–PLASTIC TORSION OF CIRCULAR SHAFTS

We now consider the torsion of circular bars of ductile materials, which are idealized as elastoplastic, stressed into the plastic range. In this case, the first two basic assumptions associated with small deformations of circular bars in torsion (see Sec. 6.2) are still valid. This means that the circular cross sections remain plane and their radii remain straight. Consequently, strains vary linearly from the shaft axis. The shearing
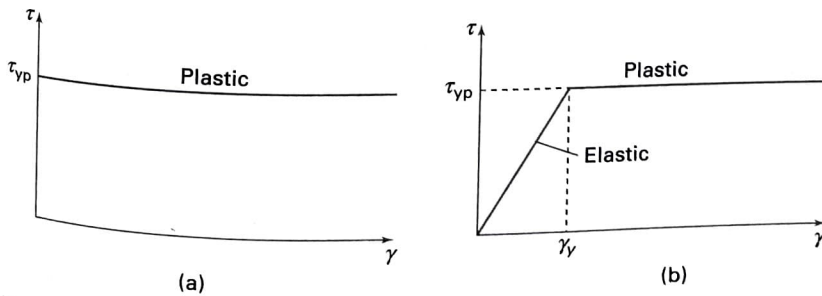

FIGURE 12.21. *Idealized shear stress–shear strain diagrams for (a) perfectly plastic materials; (b) elastoplastic materials.*

stress–strain curve of plastic materials is shown in Fig. 12.21. Referring to this diagram, we can proceed as discussed before and determine the stress distribution across a section of the shaft for any given value of the torque T.

The basic relationships given in Section 6.2 are applicable as long as the shear strain in the bar does not exceed the yield strain γ_{yp}. It is recalled that the condition of torque equilibrium for the entire shaft (Fig. 6.2) requires

$$T = \int_A \rho\tau dA = 2\pi \int_A \tau\rho^2 d\rho \qquad \text{(a)}$$

Here ρ, τ are any arbitrary distance and shearing stress from the center O, respectively, and A the entire area of a cross section of the shaft. Increasing in the applied torque, yielding impends on the boundary and moves progressively toward the interior. The cross-sectional stress distribution will be as shown in Fig. 12.22.

At the start of yielding (Fig. 12.22a), the torque T_{yp}, through the use of Eq. (6.1), may be written in the form:

$$T_{yp} = \frac{\pi c^3}{2} \tau_{yp} = \frac{J}{c} \tau_{yp} \qquad \text{(12.18)}$$

The quantity $J = \pi c^4/2$ is the polar moment of inertia for a solid shaft with radius $r = c$. Equation (12.18) is called the *maximum elastic torque*, or *yield torque*. It represents the largest torque for which the deformation remains fully elastic.

If the twist is increased further, an inelastic or *plastic portion* develops in the bar around an elastic core of radius ρ_0 (Fig. 12.22b). Using Eq. (a), we obtain that the torque resisted by the elastic core equals

$$T_1 = \frac{\pi \rho_0^3}{2} \tau_{yp} \qquad \text{(b)}$$

The outer portion is subjected to constant yield stress τ_{yp} and resists the torque,

$$T_2 = 2\pi \int_{\rho_0}^c \tau_{yp}\rho^2 d\rho = \frac{2\pi}{3}(c^3 - \rho_0^3)\tau_{yp} \qquad \text{(c)}$$
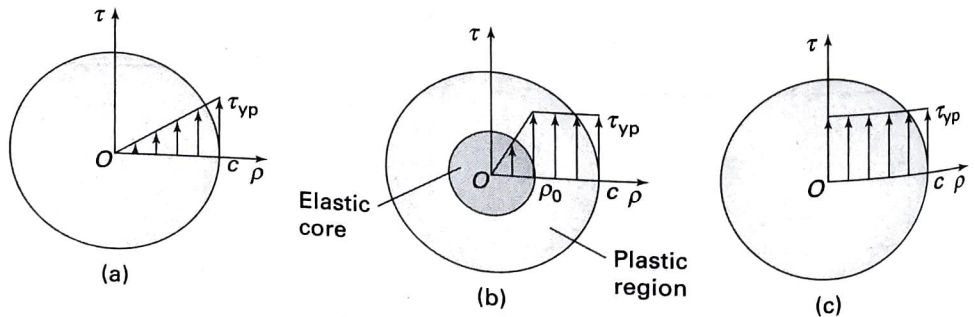

FIGURE 12.22. *Stress distribution in a shaft as torque is increased: (a) onset of yield; (b) partially plastic; and (c) fully plastic.*

The elastic–plastic or *total torque* T, the sum of T_1 and T_2, may now be expressed as follows

$$T = \frac{\pi c^3}{6}\left(4 - \frac{\rho_0^3}{c^3}\right)\tau_{yp} = \frac{4}{3}T_{yp}\left(1 - \frac{1}{4}\frac{\rho_0^3}{c^3}\right) \tag{12.19}$$

When twisting becomes very large, the region of yielding will approach the middle of the shaft and will approach zero (Fig. 12.22c). The corresponding torque T_u is the plastic, or ultimate, shaft torque, and its value from the foregoing equation is

$$T_u = \frac{2}{3}\pi c^3 \tau_{yp} = \frac{4}{3}T_{yp} \tag{12.20}$$

It is thus seen that only one-third of the torque-carrying capacity remains after τ_{yp} is reached at the outermost fibers of a shaft.

The radius of elastic core (Fig. 12.22b) is found, referring to Fig. 6.2, by setting $\gamma = \gamma_{yp}$ and $\rho = \rho_0$. It follows that

$$\rho_0 \frac{L\gamma_{yp}}{\phi} \tag{12.21a}$$

in which L is the length of the shaft. The angle of twist at the onset of yielding ϕ_{yp} (when $\rho_0 = c$) is therefore

$$c = \frac{L\gamma_{yp}}{\phi_y} \tag{12.21b}$$

Equations (12.21) lead to the relation,

$$\frac{\rho_0}{c} = \frac{\phi_{yp}}{\phi} \tag{12.22}$$

Using Eq. (12.19), the ultimate torque may then be expressed in the form:

$$T_u = \frac{4}{3}T_{yp}\left(1 - \frac{1}{4}\frac{\phi_{yp}^3}{\phi^3}\right) \tag{12.23}$$

This is valid for $\phi > \phi_{yp}$. When $\phi < \phi_{yp}$, linear relation (6.3) applies.
A sketch of Eqs. (6.3) and (12.23) is illustrated in Fig. 12.23. Observe that after yielding torque T_{yp} is reached, T and ϕ are related nonlinearly. As T approaches T_u,

FIGURE 12.23. *Torque–angle of twist relationship for a circular shaft.*

571
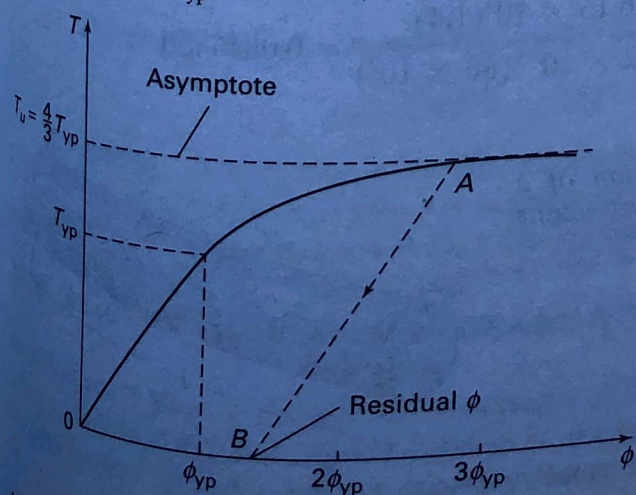
the angle of twist grows without limit. A final point to be noted, however, is that the value of T_u is approached very rapidly (for instance, $T_u = 1.32T_{yp}$ when $\phi = 3\phi_{yp}$).

When a shaft is strained beyond the elastic limit (point A in Fig. 12.23) and the applied torque is then removed, rebound is assumed to follow Hooke's law. Thus, once a portion of a shaft has yielded, *residual stresses* and *residual rotations* (ϕ_B) will develop. This process and the application of the preceding relationships are demonstrated in Example 12.12. Statically indeterminate, inelastic torsion problems are dealt with similarly to those of axial load, as was discussed in Section 12.5.

EXAMPLE 12.12   Residual Stress in a Shaft

Figure 12.24 shows a solid circular steel shaft of diameter d and length L carrying a torque T. Determine (a) the radius of the elastic core; (b) the angle of twist of the shaft; (c) the residual stresses and the residual rotation when the shaft is unloaded. *Assumption:* The steel is taken to be an elastoplastic material. *Given:* $d = 60$ mm, $L = 1.4$ m, $T = 7.75$ kN·m, $T_{yp} = 145$ MPa, and $G = 80$ GPa.

Solution We have $c = 30$ mm and $J = \pi(0.03)^4/2 = 1272 \times 10^{-9}$ m⁴.

a. Radius of Elastic Core. The yield torque, applying Eq. (12.18), equals

$$T_{yp} = \frac{J\tau_{yp}}{c} = \frac{1272 \times 10^{-9}(145 \times 10^6)}{0.03} = 6.15 \text{ kN·m}$$

Equation (12.19), substituting the values of T and τ_{yp}, gives
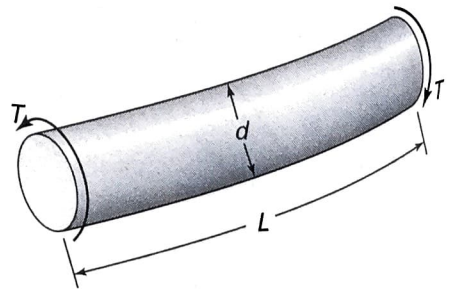
$$\left(\frac{\rho_0}{c}\right)^3 = 4 - \frac{3T}{T_{yp}} = 4 - \frac{3(7.75 \times 10^3)}{6.15 \times 10^3} = 0.22$$

Solving, $\rho_0 = 0.604\,(30) = 18.1$ mm. The elastic–plastic stress distribution in the loaded shaft is illustrated in Fig. 12.25a.

b. Yield Twist Angle. Through the use of Eq. (6.3), the angle of twist at the onset of yielding,

$$\phi_{yp} = \frac{T_{yp}L}{GJ} = \frac{6.15 \times 10^3(1.4)}{1272 \times 10^{-9}(80 \times 10^9)} = 0.0846 \text{ rad}$$

FIGURE 12.24.   *Example 12.13. Torsion of a circular bar of elastoplastic material.*
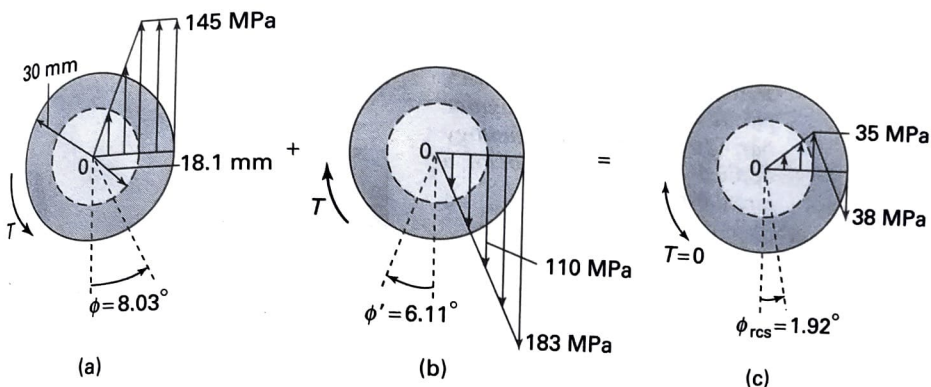
FIGURE 12.25. *Example 5.13 (continued). (a) Partial plastic stresses; (b) elastic rebound stresses; (c) residual stresses.*

Introducing the value found for ϕ_{yp} into Eq. (12.22), we have

$$\phi = \frac{C\phi_{yp}}{\rho_0} = \frac{30(0.0846)}{18.1} = 0.1402 \text{ rad} = 8.03°$$

c. *Residual Stresses and Rotation.* The removal of the torque produces elastic stresses as depicted in Fig. 12.25b, and the torsion formula, Eq. (6.1), leads to reversed stress as

$$\tau'_{max} = \frac{Tc}{J} = \frac{7.75 \times 10^3(30 \times 10^{-3})}{1272(10^{-9})} = 183 \text{ MPa}$$

Superposition of the two distributions of stress results in the residual stresses (Fig. 12.25c).
Permanent Twist. The elastic rebound rotation, using Eq. (6.3), equals

$$\phi' = \frac{TL}{GJ} = \frac{7.75 \times 10^3(1.4)}{1272 \times 10^{-9}(80 \times 10^9)} = 0.1066 \text{ rad} = 6.11°$$

The preceding results indicate that residual rotation of the shaft is

$$\phi_{res} = 8.03° - 6.11° = 1.92°$$

Comment We see that even though the reversed stresses τ'_{max} exceed the yield strength τ_{yp}, the assumption of linear distribution of these stresses is valid, inasmuch as they do not exceed $2\tau_{yp}$.

12.10 PLASTIC TORSION: MEMBRANE ANALOGY

Recall from Chapter 6 that the maximum shearing stress in a slender bar of arbitrary section subject to pure torsion is always found on the boundary. As the applied torque is increased, we expect yielding to occur on the boundary and to

573

Plastic Torsion: Membrane Analogy

FIGURE 12.26. (a) Partially yielded rectangular section; (b) membrane–roof analogy applied to elastic–plastic torsion of a rectangular bar; (c) sand hill analogy applied to plastic torsion of a circular bar.
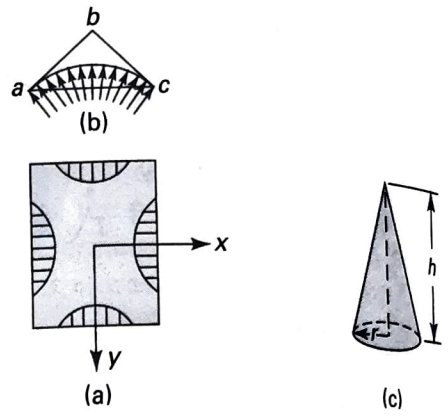
move progressively toward the interior, as sketched in Fig. 12.26a for a bar of rectangular section. We now determine the ultimate torque T_u that can be carried. This torque corresponds to the totally plastic state of the bar, as was the case of the beams previously discussed. Our analysis treats only perfectly plastic materials.

The stress distribution within the elastic region of the bar is governed by Eq. (6.9),

$$\frac{\partial^2 \Phi}{\partial x^2} + \frac{\partial^2 \Phi}{\partial y^2} = -2G\theta \tag{12.24}$$

where Φ represents the stress function ($\Phi = 0$ at the boundary) and θ is the angle of twist. The shearing stresses, in terms of Φ, are

$$\tau_{zx} = \frac{\partial \Phi}{\partial y}, \quad \tau_{zy} = -\frac{\partial \Phi}{\partial x} \tag{a}$$

Inasmuch as the bar is in a state of pure shear, the stress field in the plastic region is, according to the *Mises yield criterion*, expressed by

$$\left(\frac{\partial \Phi}{\partial x}\right)^2 + \left(\frac{\partial \Phi}{\partial y}\right)^2 = \tau_{yp}^2 \tag{12.25}$$

where τ_{yp} is the yield stress in shear. This expression indicates that the slope of the Φ surface remains constant throughout the plastic region and is equal to τ_{yp}.

Membrane–Roof Analogy

Bearing in mind the condition imposed on Φ by Eq. (12.25), the membrane analogy (Sec. 6.6) may be extended from the purely elastic to the elastic–plastic case. As shown in Fig. 12.26b, a roof *abc* of constant slope is erected with the membrane as its base. Figure 12.26c shows such a roof for a circular section. As the pressure acting beneath the membrane increases, more and more contact is made between the membrane and the roof. In the fully plastic state, the membrane is in total contact with the roof, membrane and roof being of identical slope. Whether the membrane makes partial or complete contact with the roof clearly depends on the pressure. The membrane–roof analogy thus permits solution of elastic–plastic torsion problems.

TABLE 12.1. *Torque Capacity for Various Common Sections*

Cross section	Radius or sides	Torque T_u for full plasticity
Circular	r	$\frac{2}{3}\pi r^3 \tau_{yp}$
Equilateral triangle	a	$\frac{1}{12}a^3 \tau_{yp}$
Rectangle	a, b	$\frac{1}{6}a^2(3b - a)\tau_{yp}$
	$(b > a)$	
Square	a	$\frac{1}{3}a^3 \tau_{yp}$
Thick-walled tube	b: outer	$\frac{2}{3}\pi(b^3 - a^3)\tau_{yp}$
	a: inner	

Sand Hill Analogy

For the case of a totally yielded bar, the membrane–roof analogy leads quite naturally to the *sand hill analogy*. We need not construct a roof at all, using this method. Instead, sand is heaped on a plate whose outline is cut into the shape of the cross section of the torsion member. The torque is, according to the membrane analogy, proportional to twice the volume of the sand figure so formed. The ultimate torque corresponding to the fully plastic state is thus found.

Referring to Fig. 12.26c, let us apply the sand hill analogy to determine the ultimate torque for a circular bar of radius r. The volume of the corresponding cone is $V = \frac{1}{3}\pi r^2 h$, where h is the height of the sand hill. The slope h/r represents the yield point stress τ_{yp}. The ultimate torque is therefore

$$T_u = \frac{2}{3}\pi r^3 \tau_{yp} \tag{12.26}$$

Note that the maximum elastic torque is $T_{yp} = (\pi r^3/2)\tau_{yp}$. We may thus form the ratio

$$\frac{T_u}{T_{yp}} = \frac{4}{3} \tag{12.27}$$

Other solid sections may be treated similarly [Ref. 12.7]. Table 12.1 lists the ultimate torques for bars of various cross-sectional geometry.

The procedure may also be applied to members having a symmetrically located hole. In this situation, the plate representing the cross section must contain the same hole as the actual cross section.

12.11 ELASTIC–PLASTIC STRESSES IN ROTATING DISKS

This section treats the stresses in a flat disk fabricated of a *perfectly plastic material*, rotating at constant angular velocity. The maximum elastic stresses for this geometry are, from Eqs. (8.30) and (8.28) as follows: For the solid disk at $r = 0$,

$$\sigma_\theta = \sigma_r = \frac{\rho\omega^2(3 + \nu)b^2}{8} \tag{a}$$